Energy Storage and Dissipation Notes
Note 10
March 15, 1990

High-Frequency Capacitors

D. V. Giri
Pro-Tech, 125 University Avenue, Berkeley, CA 94710

and

Carl E. Baum
Weapons Laboratory

Abstract

The object of this note is to describe certain conceptual designs in fabricating capacitors for high-frequency operation. Problems, in terms of high-frequency performance of currently used capacitors are identified and new design concepts presented. Techniques such as shorter transit times, multiple tabs for output, maximizing symmetry and lossy foils are investigated with the goal of maximizing the frequency response of the capacitor. This has led us to a dihedral $D_{2,d}$ unit capacitor, which can be strung together to form a dihedral column capacitor.

Foreword

The authors are thankful to Mr. Mike Dinallo, formerly with the BDM Corporation for valuable discussions. We are also grateful to Dr. R. L. Gardner of Mission Research Corporation for his encouragement and support.

CONTENTS

Section		Page
1.	Introduction	5
2.	Brief Review of Problems with Capacitors in Use	6
3.	Transmission-Line Model of Winding	10
4.	Multiple Tabs on Winding	15
5.	Maximizing Capacitor Frequency Response	22
6.	Dihedral Capacitors	24
7.	Radial-Transmission in a D_∞ Capacitor.	32
8.	Tab Outputs for D_N Capacitor	42
9.	Combining $D_{N,d}$ Unit Capacitors.	45
10.	Concluding Remarks	50
	References	51

LIST OF FIGURES

Figure		Page
1	Typical elemental capacitor in use	7
2	Stacking of N elemental capacitors (after they are wound) to form a unit capacitor	8
3	Capacitor measurement in a coaxial geometry	9
4	Two-plate-transmission line model of an elemental capacitor	11
5	Single and two sided tabs on foil capacitors	16
6	Short tabs for lowering the tab inductance (in contrast with longer tabs in figure 2a)	17
7	Once or more tabs at opposite edges	17
8	Multiple tabs to divide up the current paths	17
9	Conventional spiral winding of the capacitor with a symmetry plane P_1	19
10	Spiral winding with two symmetry planes P_1 and P_2	19
11	Spiral winding with a rotation axis ($\vec{1}_0$) and symmetry plane P_1	20
12	C_2 capacitors	26
13	$D_{2,d}$ group	27
14	$D_{2,t}$ group	27
15	$D_{3,t}$ or $D_{3,d}$, dihedral symmetry group with 12 elements (shapes of plates are not unique)	29
16	$D_{4,t}$ or $D_{4,d}$, dihedral symmetry group with 16 elements (shapes of plates are not unique)	29
17	Capacitor belonging to the dihedral D_N symmetry group	30
18	$D_{N,d}$ dihedral capacitor made of M number of circular A and B plates each, with tabs	31

19	$D_{N,t}$, dihedral capacitor made of N_A number of circular A and $(N_A - 1)$ number of circular B-plates, with tabs	31
20	Disk capacitor and cylindrical coordinates (Ψ, ϕ, z) for analyzing radial transmission	33
21	Normalized input impedance of a circular disk (or D_∞ - dihedral) capacitor	36
22	$D_{2,d}$ capacitor	43
23	$D_{2,t}$ capacitor	43
24	Two ways of bending the tabs, both of which can be applied to $D_{2,d}$ and $D_{2,t}$ above	43
25	Stringing of $D_{2,d}$ capacitors to form a column capacitor	46
26	Column of $D_{2,d}$ capacitors	47
27	A column of $D_{2,d}$ capacitors for the two cases of N_c even and odd	48

1. Introduction

Capacitors have many applications ranging from modern electronic circuits to energy-storage devices. They are also used over a wide range of frequencies and operating voltages. In the context of EMP generators, [1,2] peaking capacitors are employed in pulse shaping (circuit function) as well as in transporting a fast wave (wave function). For a satisfactory performance, the peaking capacitor is required to function at increasingly higher frequencies. In other words, owing to the nature of their construction, peaking capacitors inevitably display both short-circuit and open-circuit types of resonances, and it is desirable to make the first open-circuit resonant frequency as high as practical. The short-circuit resonances where the peaking capacitor behaves electrically like a low-valued resistor do not create any problem in transporting the fast wave. For instance, in a Marx pulser, after the closure of the output switch, the peaking capacitor is required to behave like a "conductor" and open-circuit resonances are undesirable. This is the basic problem and our present interest is to outline a few design concepts for fabricating capacitors for high-frequency applications.

2. Brief Review of Problems with Capacitors in Use

A typical example of an elemental capacitor in use is shown in figure 1. It consists of two metallic foils separated by a single or multiple layers of dielectric strips. The metallic foils have length l, and width w and are separated by a distance d. Typical dimensions are 0.5 to $1.2m$ for l, about $0.1m$ for w and 50 to $100\mu m$ for d. For example, for an assumed $\varepsilon_r = 4.5$, $l = 0.5m$, w = $0.1m$ and $d = 50\mu m$, an approximate value for the elemental capacitor is given by

$$C = \varepsilon_0 \varepsilon_r \frac{\mathrm{w}l}{d} \simeq 40nF \tag{1}$$

which is a fairly typical number. Such elemental capacitors are required to operate nominally up to $10kV$ (say) and at high frequencies. These elemental capacitors of figure 1 are "wound" after metallic tabs are inserted and then stacked to form a unit capacitor. This is illustrated in figure 2. The mechanical details of fabrication and packaging are not of present interest, since our aim is to evaluate and improve the electrical performance.

Unit capacitors can be series connected to form a capacitor arm. Unit capacitors, such as the ones illustrated here, have been experimentally evaluated in the past by several researchers. The measurements have been done, for example by applying a voltage to a capacitor assembly with respect to a ground plane and recording the output voltage across a load at the other end. Another experimental scheme involved using a coaxial geometry where the capacitor is used as the "inner conductor" of an approximately 50Ω coaxial transmission line (see figure 3). With the coaxial geometry [3], similar measurement of $(\tilde{V}_{out}/\tilde{V}_{in})$ were made as a function of frequency.

One can make the following observations from the past experimental evaluations of the capacitors

1. $(\tilde{V}_{out}/\tilde{V}_{in})$ is zero at DC as one would expect, (or $\tilde{Z}_{in}$ tends to infinity).
2. The problem frequencies are where $(\tilde{V}_{out}/\tilde{V}_{in})$ becomes small or the input impedance $\tilde{Z}_{in}$ becomes high.
3. Resonances, described above occur at 10's of MHz frequencies.
4. There can be significant losses as more and more unit capacitors are series connected.
5. There is reasonably good correlation between the results obtained from two-wire line and coaxial test geometries.

The performance problems, especially the undesirable resonances can lead to more serious problems in the intended application of such capacitors [4]. One needs to think of improved capacitors with better high-frequency performance.

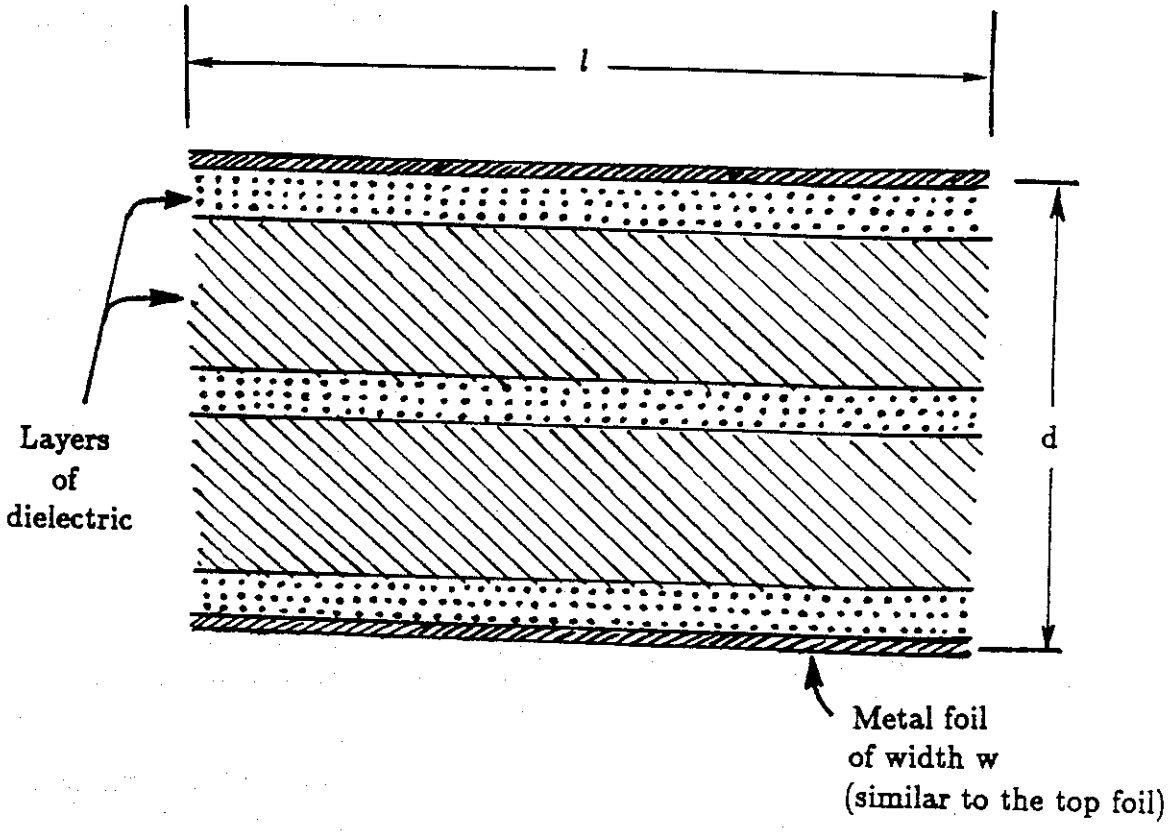

Figure 1. Typical elemental capacitor in use

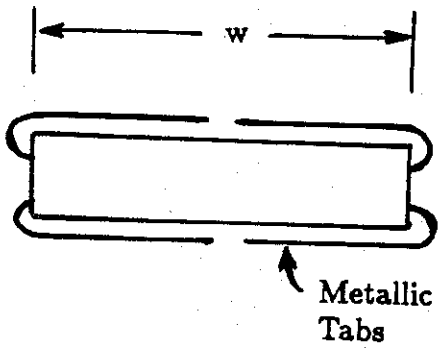

a) Elemental capacitor after it has been "wound"

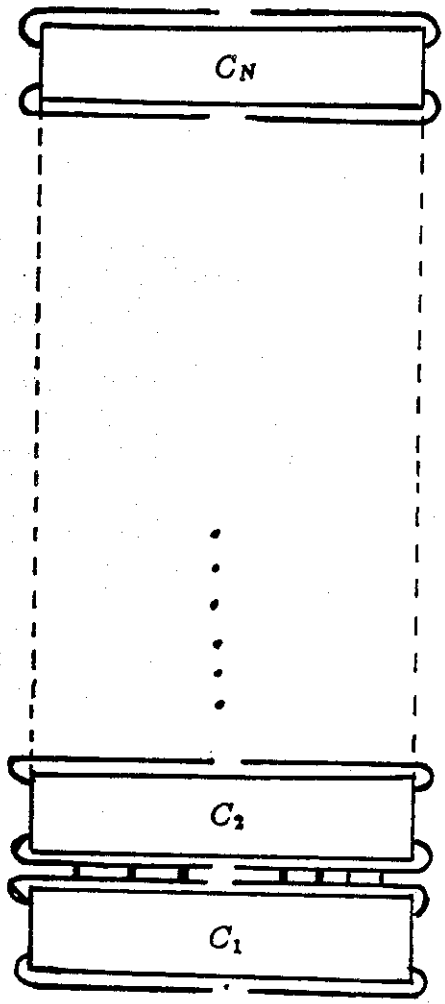

b) Stacking of elemental capacitors

Figure 2. Stacking of N elemental capacitors (after they are wound) to form a unit capacitor

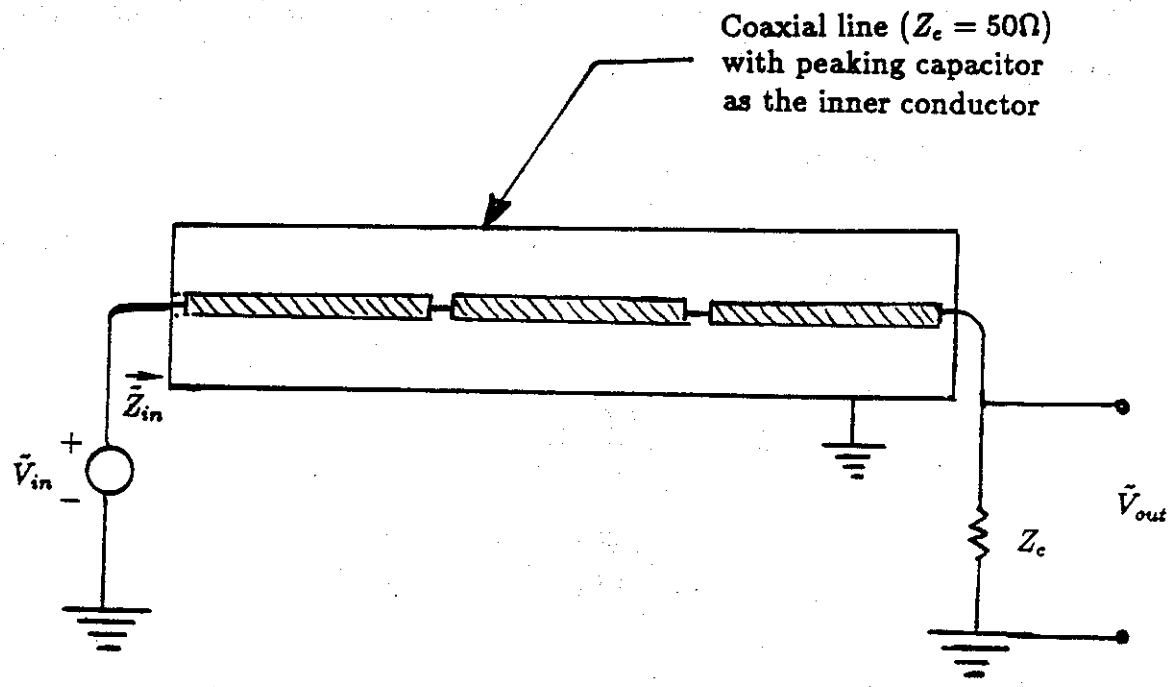

Figure 3. Capacitor measurement in a coaxial geometry

3. Transmission-Line Model of Winding

One can easily formulate a two-conductor transmission line model of an elemental capacitor shown in figure 1. The two conductors are the metallic foils or "plates", and the transmission line formed by the foils is illustrated in figure 4. The two foils are separated by a dielectric medium with a relative dielectric constant of ϵ_r. Note that the metallic foils can be lossless ($\sigma = \infty$) or lossy (σ is adequately high, but finite). We can define an input impedance $\tilde{Z}_{in}$ for such a capacitor and formulate expressions for it under both lossless and lossy situations.

A. Lossless foil capacitor.

When the metallic foils are lossless, i.e., the conductivity $\sigma = \infty$, the input impedance of the capacitor can be written as

$$\begin{aligned} \tilde{Z}_{in} &= \sqrt{\frac{Z'}{Y'}}\ \frac{1+e^{-2\gamma l}}{1-e^{-2\gamma l}} \\ &= \sqrt{\frac{Z'}{Y'}}\frac{cosh(\gamma l)}{sinh(\gamma l)} = \sqrt{\frac{Z'}{Y'}}coth(\gamma l) \end{aligned} \tag{2}$$

where

$$Z' \equiv \text{impedance per unit length} = \mathrm{sL}' \simeq s\mu_0 d/\mathrm{w}$$

$$Y' \equiv \text{admittance per unit length} = \mathrm{sC}' \simeq s\epsilon \mathrm{w}/d$$

$$\gamma \equiv \text{propagation constant} = \mathrm{s/v} = \sqrt{Z'Y'}$$

$$l, \mathrm{w}, d \equiv \text{length, width and separation of the foils}$$

$$\mu_0 \equiv \text{permeability of free space}$$

$$\epsilon \equiv \text{permittivity of the dielectric} = \epsilon_0\epsilon_r$$

$$\epsilon_0 \equiv \text{permittivity of free space}$$

$$\mathrm{v} \equiv \text{speed of light in the dielectric} = \frac{1}{\sqrt{\mu_0\epsilon}}$$

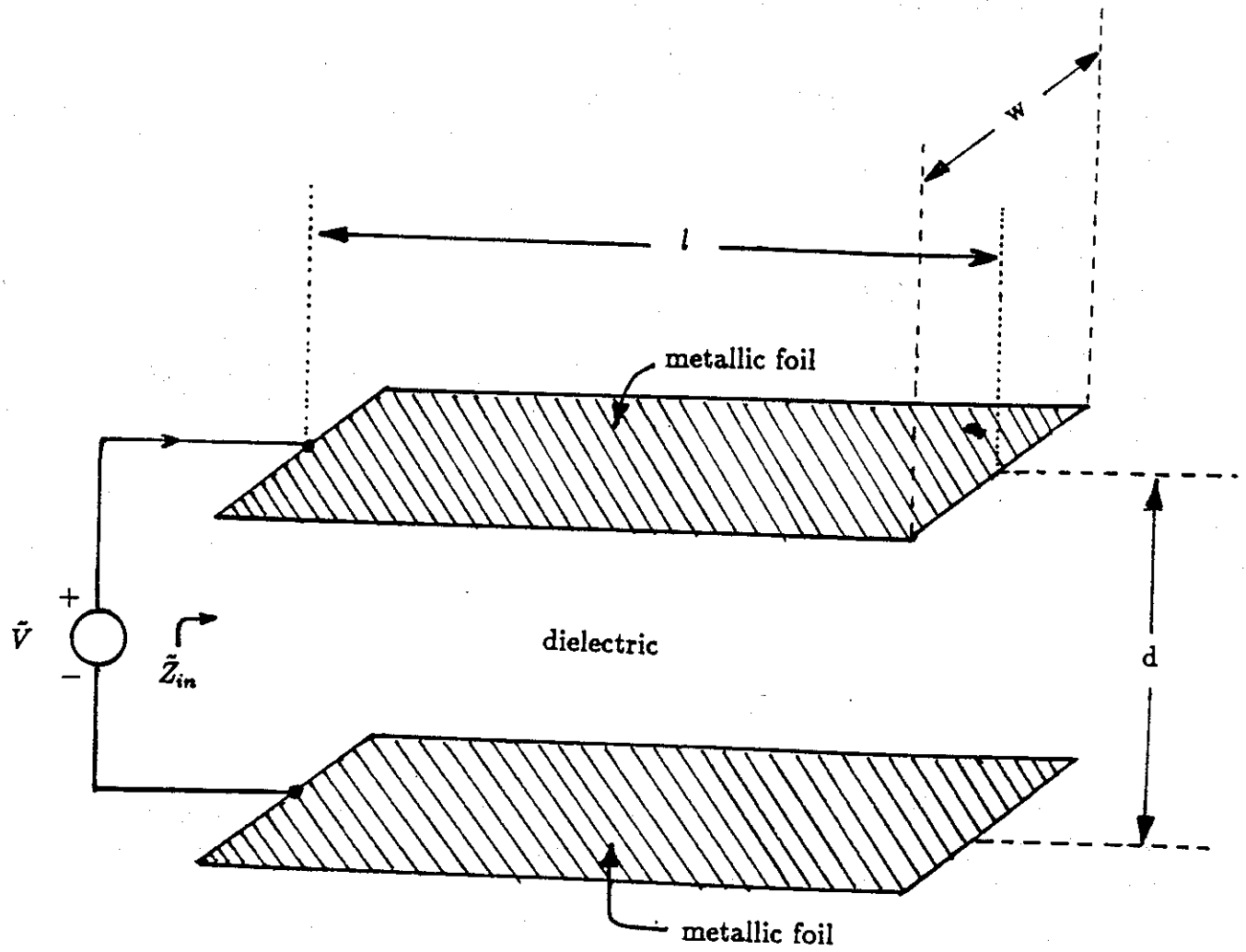

Figure 4. Two-plate-transmission line model of an elemental capacitor

The input impedance now becomes

$$\tilde{Z}_{in} = \sqrt{\frac{Z'}{Y'}}\, coth(\gamma l) = \frac{\sqrt{Z'Y'}}{Y'}\, coth(\gamma l)$$

$$= \frac{\gamma}{sC'}\, coth(\gamma l) = \frac{\gamma l}{sC}\, coth(\gamma l) \tag{3}$$

where $C = C'l = \varepsilon\, \mathrm{w}l/d \equiv$ foil capacitance

We can observe that at low frequencies (i.e. $\gamma l \to 0$), $\tilde{Z}_{in}$ becomes $\tilde{Z}_{ideal} = (sC)^{-1}$ as required. One can also specialize the above expression by setting $s = j\omega$ and $\gamma = jk$ leading to

$$\frac{\tilde{Z}_{in}}{Z_{ideal}} = sC\tilde{Z}_{in} = (\gamma l) coth(\gamma l) \tag{4}$$

or

$$\frac{\tilde{Z}_{in}}{Z_{ideal}} = j\omega C\tilde{Z}_{in} = (kl) cot(kl) \tag{5}$$

The above expression exhibits a first short-circuit resonance at $kl = \pi/2$ and a first unwanted open-circuit resonance at $kl = \pi$. Recall that (kl) for the present case of lossless foils (i.e., perfect conductor foils) is simply given by

$$kl = \frac{\omega l}{\mathrm{v}} = \frac{\omega}{c}\, l\sqrt{\varepsilon_r} \tag{6}$$

so that

$$\frac{\tilde{Z}_{in}}{\tilde{Z}_{ideal}} = \left(\frac{\omega}{c}\, l\sqrt{\varepsilon_r}\right) cot\left(\frac{\omega}{c}\, l\sqrt{\varepsilon_r}\right) \tag{7}$$

The above expression is real and displays the first unwanted resonance when the argument of the cotangent becomes π. This unwanted resonant frequency f_r is given by

$$f_r = \frac{c}{2l\sqrt{\varepsilon_r}} \tag{8}$$

which is about 70 MHz if $l = 1m$ and $\varepsilon_r = 4.5$. Incidentally, the first short-circuit resonance which occurs when $(kl = \pi/2)$ corresponds to a frequency of 35 MHz and does not lead to any significant problem.

We can now introduce losses in the foils which tend to damp the unwanted resonances.

B. Lossy foil capacitor.

Let us say the foils are made of lossy material whose conductivity is σ and permeability $\mu = \mu_0\mu_r$. The foils then introduce additional series impedance per unit length according as

$$\tilde{Z}' = sL' + 2\frac{\tilde{Z}_s}{w} \tag{9}$$

where the surface impedance $\tilde{Z}_s$ is given by

$$\tilde{Z}_s \simeq \sqrt{s\mu/\sigma} \text{ (dimension } \Omega \text{ and sometimes called } \Omega \text{ per square)} \tag{10}$$

The propagation constant γ is now given by

$$\gamma = \sqrt{Z'Y'} = s\sqrt{L'C'}\sqrt{1+\frac{2Z_s}{s\mu_0 d}}$$

$$\frac{s}{C}\sqrt{\varepsilon_r}\left[1+\frac{1-j}{d}\sqrt{\frac{2\mu_r}{\omega\mu_0\sigma}}\right]^{\frac{1}{2}} \tag{11}$$

The normalized input impedance is still given by

$$\frac{\tilde{Z}_{in}}{\tilde{Z}_{ideal}} = (\gamma l)coth(\gamma l) \tag{12}$$

where γ is given by (11) for the lossy foils.

As before setting $s = j\omega$ and $\gamma = jk$, we can write for the case of lossy foils

$$\left|\frac{\tilde{Z}_{in}}{\tilde{Z}_{ideal}}\right| = (kl)cot(kl) \tag{13}$$

where

$$kl = \frac{\omega\, l}{c}\sqrt{\varepsilon_r}\left[1+\frac{1-j}{d}\sqrt{\frac{2\mu_r}{\omega\mu_0\sigma}}\right]^{\frac{1}{2}} \tag{14}$$

(kl) can also be written in terms of the skin depth d_s in the foils as

$$d_s = \sqrt{\frac{2}{\omega\mu\sigma}} \tag{15a}$$

$$kl = \frac{\omega\, l}{c}\sqrt{\epsilon_r}\left[1+(1-j)\mu_r\frac{d_s}{d}\right]^{\frac{1}{2}} \tag{15b}$$

The above equation is consistent with and reduces to (6) under lossless case of $\sigma = \infty$ or $d_s = 0$.

In concluding this section, it is observed that unwanted resonances do exist in the foil capacitors and they can be damped to some extent by using lossy materials for the foils. Typically aluminum foils are used in the fabrication and improvement (i.e., damping of unwanted resonance) can be obtained by using lossy material such as lead, iron or carbon-coated foils.

4. Multiple Tabs on Winding

The elemental capacitors are interconnected by means of metallic tabs, whose inductance can also influence resonances. It is desirable to reduce the tab inductances. A single tab on each foil of the capacitor is shown in figure 5a. In this configuration, it is noted that the larger transit time t_2 governs the lower undesirable frequency.

Tab inductances can be reduced in several ways, e.g.,

a) tabs on both sides of foils as in figure 5b

b) shorter tabs as in figure 6

c) one or more tabs at the edges as in figure 7

d) multiple tabs as in figure 8

When the tabs are situated at the opposite edges as in figure 5b the mutual inductance between them is lower, because of increased separation. In figure 5b, if the tabs were placed at the center of the foil, the unwanted resonant frequency will double in value and the $\tilde{Z}_{in}$ at this resonance will be halved also, because of the parallel combination of the two sections. Shorter tabs as in figure 6 can lower the tab inductance and have been effectively employed in some recent fabrication methods. Typically tabs tend to be long and narrow metallic strips and lowering the length is always beneficial in lowering the inductance.

Multiple tabs at the opposite edges as indicated in figure 8 is also an efficient way of dividing the current path lengths and lowering the tab inductances. It is noted that in the case of multiple tabs on each foil, when the capacitor is wound, the tabs on each foil line up and can be connected for good electrical contact.

If for example we consider N tabs (equally spaced) with a spacing of $2\Delta l$, at distances $l_n (n = 1, 2...N)$ from one end of the foil according as

$$l_n = \frac{2n-1}{N}\Delta l \text{ and } \Delta l = \frac{l}{2N} \tag{16}$$

In this case, the transmission line model considered above is applicable to each of the 2N elementary capacitors, so that the input impedance of the nth section is given by

$$\tilde{Z}_{in}^{(n)} = \frac{1}{j\omega C_n}(k\Delta l)cot(k\Delta l) \tag{17a}$$

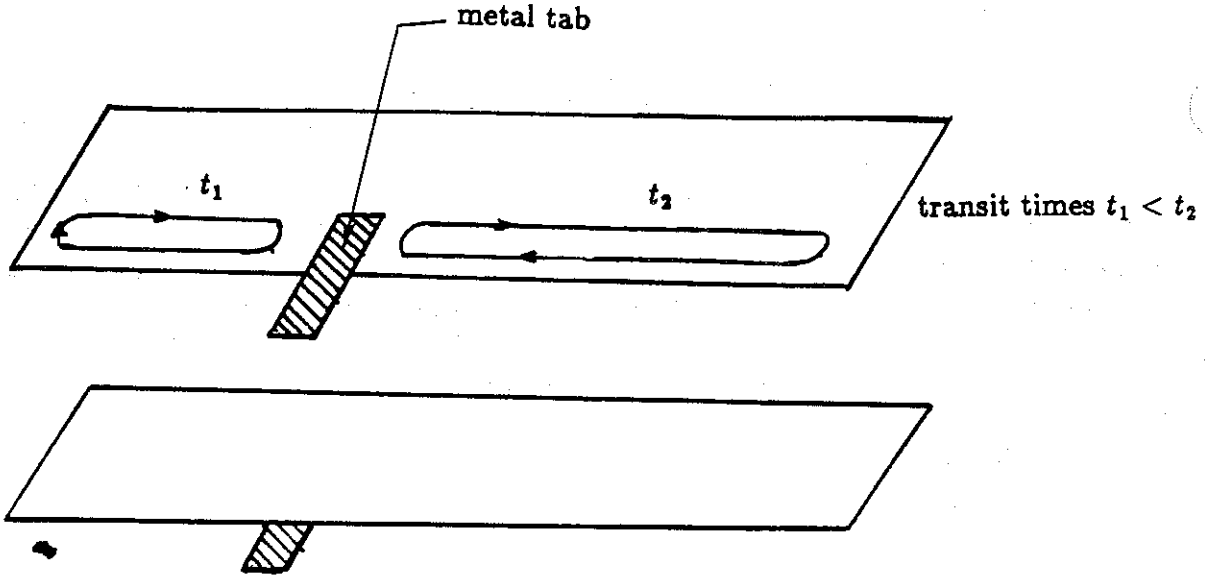

a) Single sided tabs on each foil.

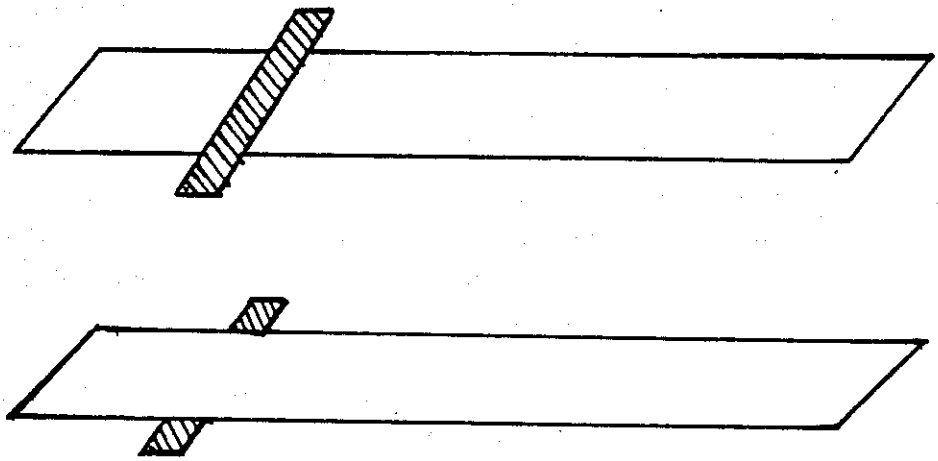

b) Two sided tabs for lower tab inductance (parallel combination of two single sided tab inductances).

Figure 5. Single and two sided tabs on foil capacitors

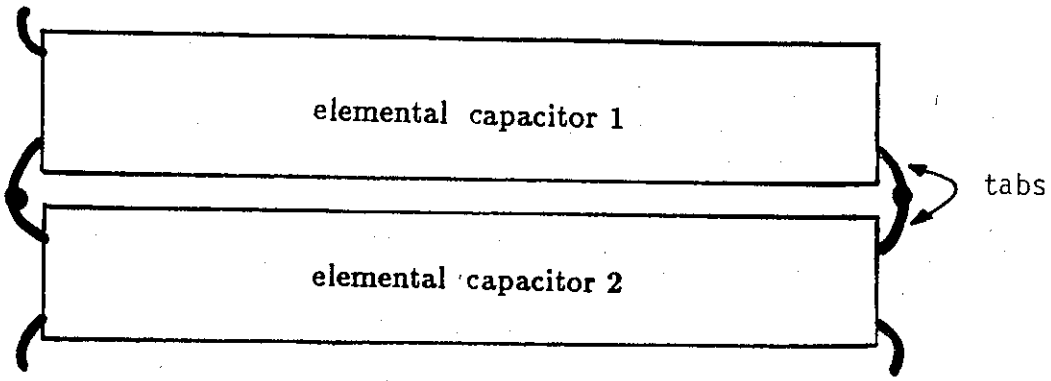

Figure 6. Short tabs for lowering the tab inductance (in contrast with longer tabs in figure 2a)

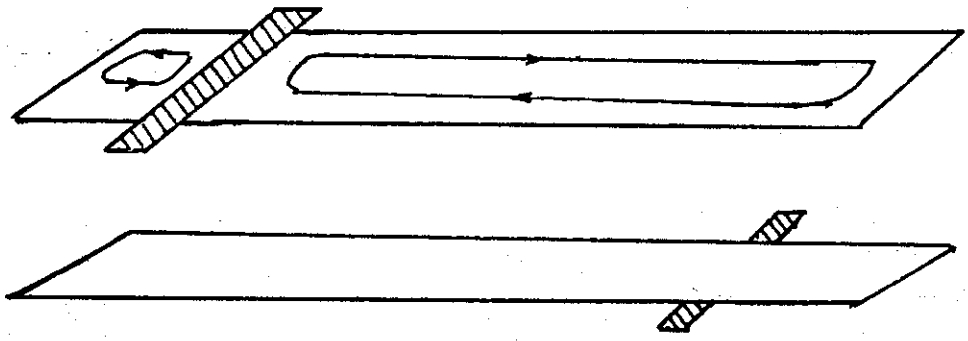

Figure 7. Once or more tabs at opposite edges

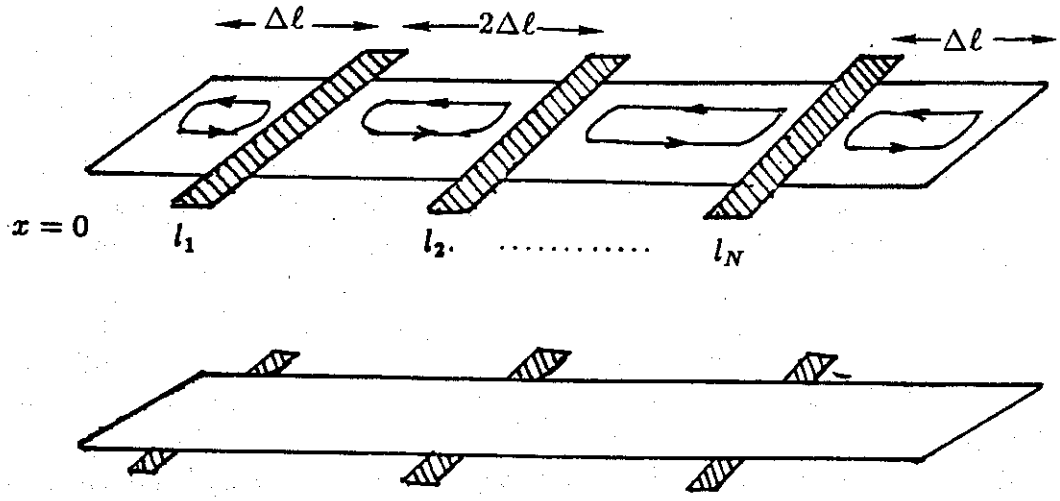

Figure 8. Multiple tabs to divide up the current paths

$$C_n = \frac{\epsilon w \Delta l}{d} \tag{17b}$$

C_n above is the capacitance of the nth section. Since there are 2N such sections in parallel, the net input impedance is a parallel combination of $\tilde{Z}_{in}^{(1)}, \tilde{Z}_{in}^{(2)}, \tilde{Z}_{in}^{(3)}, \tilde{Z}_{in}^{(4)} ....., \tilde{Z}_{in}^{(2N)}$.

If the N tabs are equally spaced with a spacing of (l/N), of course the above value of net impedance simply $\frac{1}{2N}$ times the input impedance of a single section according as

$$\begin{aligned} \tilde{Z}_{in} &= \frac{1}{2N} Z_{in}^{(n)} \quad \text{any n} \\ &= \frac{1}{2N} \frac{1}{j\omega C} \left(\frac{kl}{2N}\right) cot \left(\frac{kl}{2N}\right) \end{aligned} \tag{18}$$

From the above expression, one can also observe that for an open-circuit resonance (unwanted), the resonant half wavelength is $(l/2N)$.

With regard to the winding of the capacitor, the conventional manner of winding is shown in figure 9. In addition, two alternate winding techniques are shown in figures 10 and 11. The conventional spiral winding (figure 9) will be an R_1 capacitor if one uses two-sided tabs on both foils. R_1 denotes a reflection symmetry property [5], in particular reflection through the symmetry plane P_1. The symmetries in such capacitors involve rotation, reflection and combinations of rotations and reflections. In general, there is no translational symmetry [5] and hence these capacitors belong to the point symmetry group. We introduce the symmetry group notations here but their significance is discussed in much greater detail in later sections.

Figure 10 shows that both ends of the capacitor are wound with a symmetry plane in the center. There is a rotation symmetry and in the symmetry group notation, figure 10 is $C_{2,a}$ with 4 elements which are identity, π rotation about $\vec{1}_0$ and reflections through P_1 and P_2. Because of the two symmetry planes, only symmetric modes (symmetric with respect to both planes)[6, 7 and 8] couple to the output in this type of capacitor and the anti-symmetric modes of currents or charges are essentially decoupled or are orthogonal to the output.

On the other hand, in figure 11, we have a single symmetry plane P_1 in addition to a 2-fold symmetry or C_2 rotation axis. A good summary description of rotation and reflection symmetry group elements can be found in [9, 10]. Figures 11a illustrates one way of winding from the two ends. Figure 11b is similar to figure 11a and indicates a completed winding. Yet another possible way of winding is illustrated in figure 11c. "The winding from the middle" is not possible with the spiral winding of figure 10, since in figure 10, there is only one direction of rotation as opposed to two in the winding of figure

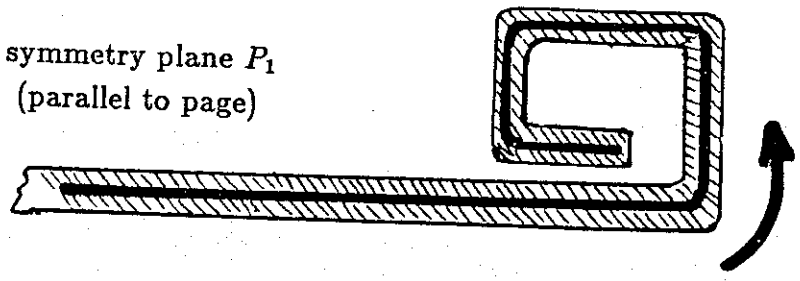

Figure 9. Conventional spiral winding of the capacitor with a symmetry plane P_1

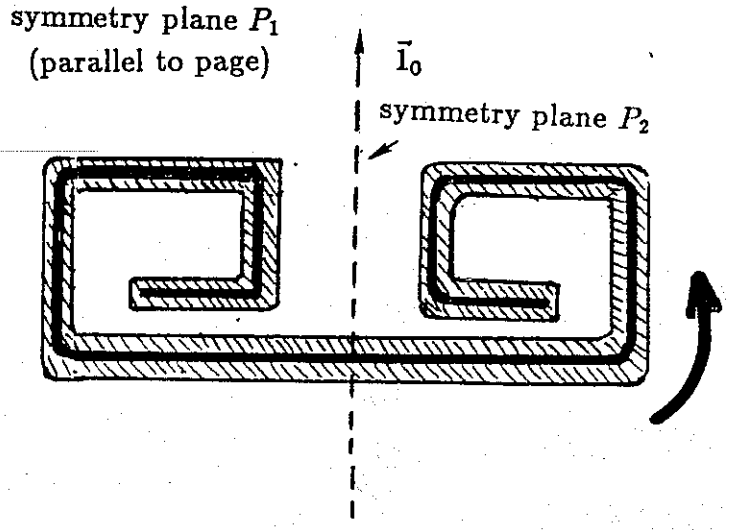

Figure 10. Spiral winding with two symmetry planes P_1 and P_2

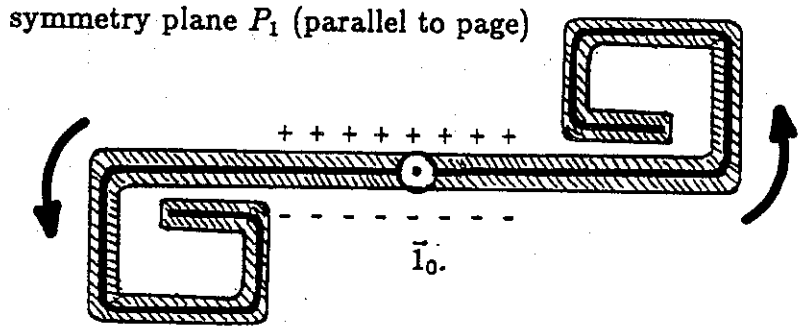

a) C_2 rotation symmetry in spiral winding
with a symmetry plane P_1

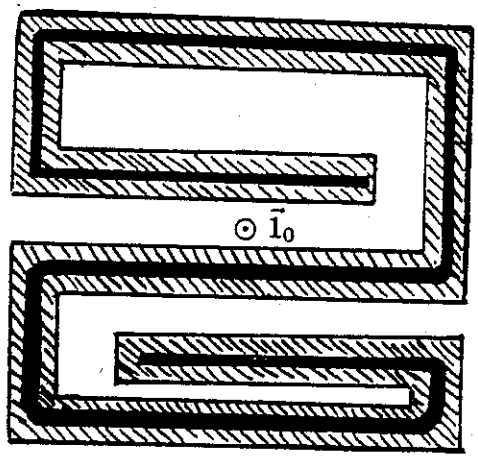

b) winding from the ends
(same as in (a) above)

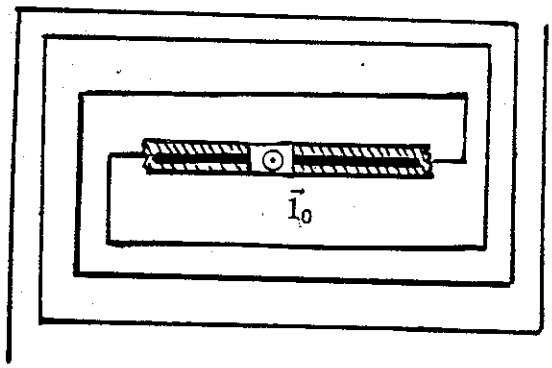

c) winding from the middle

Figure 11. Spiral winding with a rotation axis ($\vec{I}_0$) and symmetry plane P_1

11a. With reference to figure 11a, there could be many turns and we have only shown two turns for illustration. It is a $C_{2,t}$ symmetry group if we place two-sided tabs on foils and the four elements are identity, $(C_2)_1$, plus both of these combined with (R_1) reflection. These notations of symmetry groups will be clarified in later sections.

In general, the object of introducing symmetries is that the system response (e.g., capacitor current or charge) can be broken into sub-groups that are mutually exclusive (or non-interacting) and hence it becomes feasible to selectively eliminate one or the other set of resonances. In doing so, one can obtain improved high-frequency performance from the capacitors.

5. Maximizing Capacitor Frequency Response

The capacitor will be useful up to a frequency f_h where the first unwanted resonance makes the input impedance unacceptably large. If the capacitor is used in a transient application and the applied pulse has significant spectral content beyond the first unwanted resonance of the capacitor this can lead to spectral problems in devices in which the capacitor is installed. There exists a definite need to maximize the frequency response of the capacitor. We can list the techniques for maximizing the frequency response, as

a) short transit times
b) multiple tabs for output
c) maximize symmetry
d) lossy foils

Each of the above technique is briefly discussed below.

A. Short transit times

It is desirable to place the tab(s) such that transit times from all foil locations to nearest tabs are minimized. Current flow patterns on the foils themselves can lead to unwanted resonances and hence their path lengths should be minimized. Length to width ratio (l/w) can also influence the transit times. It would then appear desirable to have (l/w) of the order of unity for a given foil area. This would result in smaller transit times for resonating currents. This feature can be investigated experimentally. For a fixed (l/w), (l/w) can be varied to determine if the resonant frequency is indeed the highest for (l/w) around unity.

B. Multiple tabs for output

This subject was briefly discussed in the previous section. Multiple tabs on each foil help in lowering the net tab inductance. This is because of the parallel combination of individual tab inductances. Multiple tabs also break-up the current paths and consequently an result in an improved high frequency performance. Smaller current paths on the foil lead to shorter transit times and higher resonant frequencies. Figure 8 earlier had illustrated this effect. The multiple tabs are so positioned that when the capacitor is fully wound, the corresponding tabs line up. The tabs then are connected so that they are in good electrical contact. That is all the tabs in top foil are connected together and likewise for all the tabs on the bottom foil.

C. Maximizing symmetry

One could look at the capacitor as a system with certain internal characteristics on which there are certain current/charge modes. These modes can be decomposed into

subsets. By maximizing symmetry in the capacitor construction, one can selectively excite or eliminate certain modes. Crudely, one might say that certain modes are not supported because of the tab-coupling geometry. In other words, some modes couple to the output and some others (the unwanted ones) are orthogonal to the output and hence decoupled from it. So, maximizing symmetry in the capacitor can eliminate certain modal functions and thus improve or enhance the bandwidth. For example, with the winding of figure 10 where two symmetry planes are present, the anti-symmetric modes will be absent in the output, if they are absent in the input.

D. Lossy foils

In the transmission line model formulated in an earlier section, we saw the effect of a lossy foil in damping out the resonances of the capacitor. So, by a proper choice of foil material such as carbon coated metal, or lead or iron one can reduce the "Q" of the unwanted resonance. This has been observed mathematically and is also arguable from physical considerations. Certain amount of losses in the foil are thus seen to be beneficial in improving the capacitor performance.

We can now proceed to investigate the symmetry considerations in the following section.

6. Dihedral Capacitors

In constructing the capacitors and interconnecting several of them to form a unit capacitor, we have already observed that the concept of maximizing the symmetry helps in improving the high-frequency performance of the capacitors. Symmetry comes in many forms, such as rotation, reflection and combinations there of. We are restricting ourselves to point symmetry groups, since the capacitor is a finite sized object and has no translational symmetry. Symmetry groups have wide applications in physics and chemistry [5]. For example, the classification of a multiatomic molecule is related to its symmetry. Also, the underlying microscopic structure of crystals is related to the symmetry of their external macroscopic form. In the present context, we can build a unit capacitor comprising of many foil capacitors and require certain symmetry properties to enhance its high-frequency performance.

The symmetry of a body or an object is described by the set of all transformations (such as rotation, reflection, translation, etc.) which preserve the distance between all pairs of points of the body or the object and result in a replication of the body. In other words, after the transformation, say rotation, the body is brought into coincidence with itself. An example of such a symmetry group is C_N which means there is one N-fold symmetry axis in the body. Furthermore, the body is replicated by a rotation of $\phi = 2\pi/N$ (N is an integer) about the single, N-fold symmetry axis. A trivial example is if N = 1, we have replicated the body by a rotation of 2π about the symmetry axis. This is an identity transformation. Hence, identity is an essential element of all symmetry groups.

Once again, in the present context, we are seeking to apply symmetry considerations to a flat or "unwound" capacitor. We are seeking to break up the winding into an equivalent set of stacked (parallel) capacitors that allows higher symmetries. In addition, winding may shift the unwanted resonance downward, possibly due to enhanced mutual inductances and capacitors. Consequently, we are investigating "flat" capacitors that can be stacked in parallel to form a single unit capacitor.

Returning to the symmetry groups, C_N is a group with a single N-fold rotation axis $\vec{1}_0$. If in addition to this rotation axis, a group has a system of 2-fold axes at right angles to $\vec{1}_0$, one gets a dihedral group D_N. So, while C_N is uniaxial $(\vec{1}_0)$, D_N has $\vec{1}_0$ and $\vec{1}_1, \vec{1}_2, ...\vec{1}_N$ system of axes, where $\vec{1}_n$ is perpendicular to $\vec{1}_0$ for $n = 1, 2, 3....N$. It is also noted that the D_N group has $2N$ elements, including the identity. Hammermesh [5] has also shown that D_N is not commutative for $N \geq 3$ and it is commutative (or abelian) for N = 1 and 2.

One also has axial (R_a) and transverse (R_t) reflections about certain symmetry planes. In addition, there could be diagonal symmetry planes resulting in a reflection element (R_d).

Next, we may consider symmetry groups containing rotation reflections, or equivalently, adjunction of reflections to C_N. This is perhaps best illustrated with examples.

Figures 12a and 12b are simple examples of adjunction of reflections to C_2, consisting of N_A number of A type plates and N_B number of B type plates. The difference being, in figure 12a $N_A = N_B$ and in figure 12b, $N_A = N_B + 1$. If we use the direct product symbol $\otimes$ to denote adjunction, we can write

$$C_{2,t} = C_2 \otimes R_1 \tag{19}$$

$$C_{2,a} = C_2 \otimes R_x \qquad x = 1 \text{ or } 2 \tag{20}$$

The adjunction means that the composite group has all elements of both groups and their mutual or cross products. The 't' and 'a' in the subscript denote "transverse" and "axial" corresponding respectively to "horizontal" and "vertical" in [5]. Both these groups are commutative and each of them contains 4 elements as noted below

4 Elements of $C_{2,t}$	4 Elements of $C_{2,a}$
1. identity (1)	1. identity 1
2. C_2 rotation about $\vec{1}_1$	2. C_2 rotation about $\vec{1}_2$
3. reflection through plane $P_1(R_1)$	3. reflection through planes P_1 or P_2, i.e., $R_1 \text{or} R_2$
4. C_2 above plus reflection R_1	4. C_2 above plus reflections R_1 or R_2

In this special case, note that the N-fold axis $\vec{1}_0$ is only 1-fold. In this sense, it can be considered as dihedral D_1 since there is one C_1 axis ($\vec{1}_0$) plus one C_2 axis which is at right angles to C_1. Hence it is a degenerate D_1- like group with 4 elements.

We can now illustrate the N = 2 or D_2 dihedral group shown in figures 13 and 14. Once again the difference between figures 13 and 14 is in the number of A and B plates. In figure 13, $N_A = N_B$ and in figure 14, $N_A = N_B + 1$ as before.

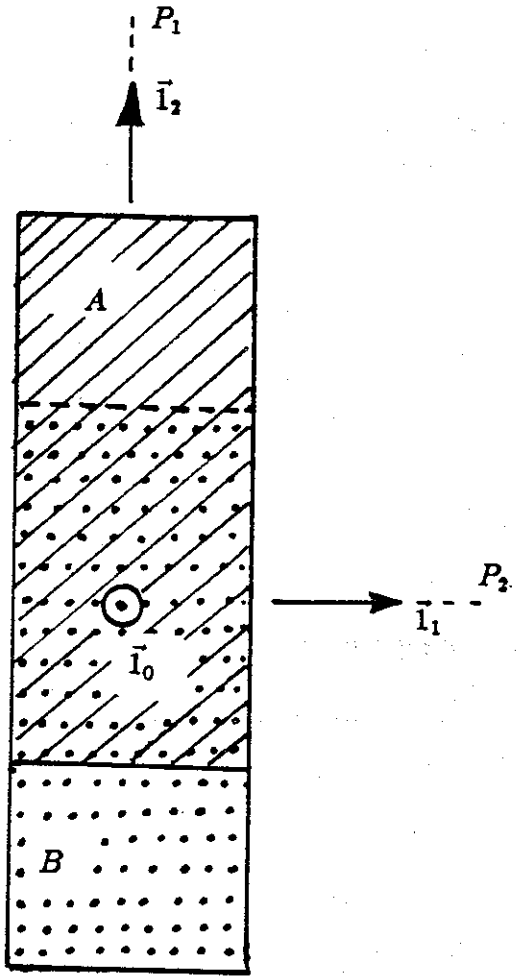

Plane P_0 is parallel to paper

Figure 12a. $C_{2,t}$ group ($\vec{l}_1$ axis)
($N_A = N_B$)
also $D_{1,a}$($\vec{l}_0$ axis)

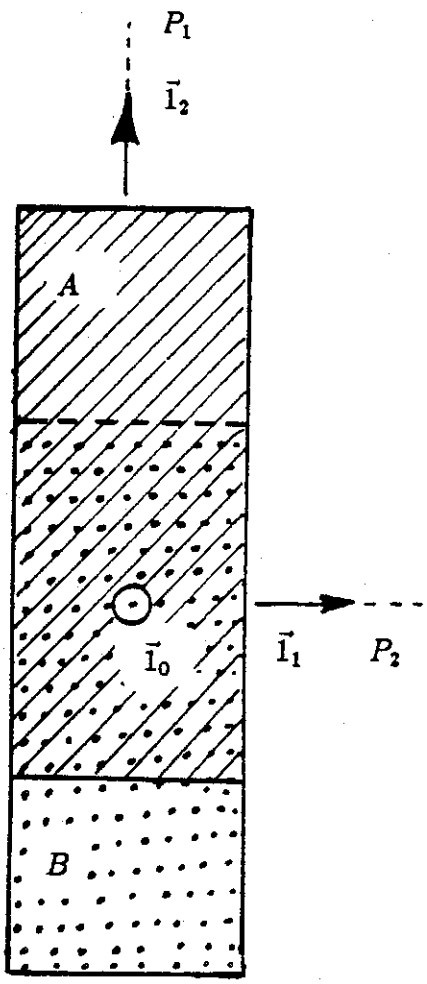

Plane P_0 is parallel to paper

Figure 12b. $C_{2,a}$ group ($\vec{l}_2$ axis)
($N_A = N_B + 1$)
also $D_{1,t}$($\vec{l}_0$ axis)

Figure 12. C_2 capacitors

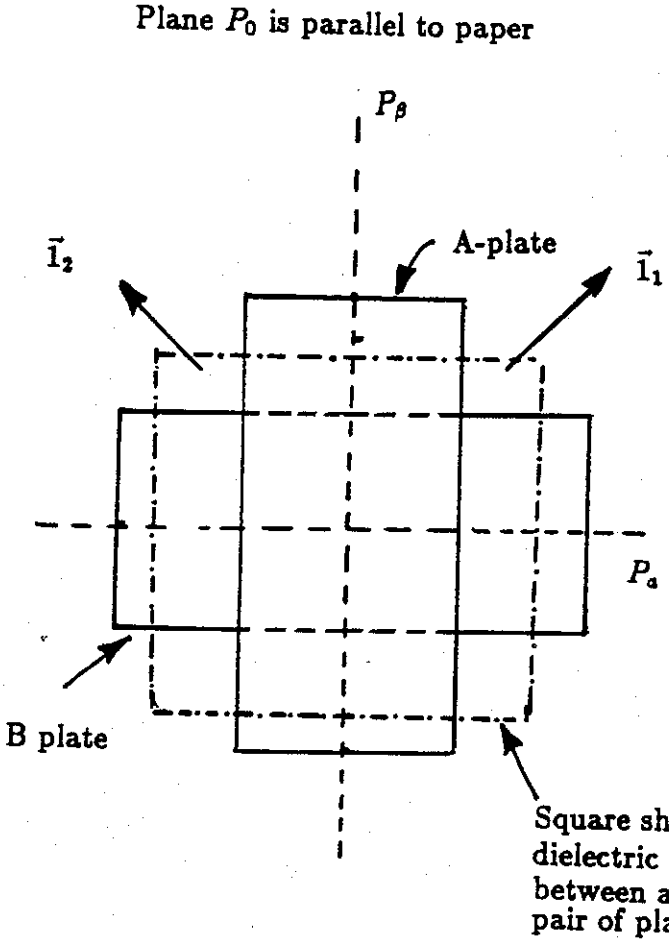

Figure 13. $D_{2,d}$ group
$(N_A = N_B)$
Type A plate on top
Type B plate on bottom

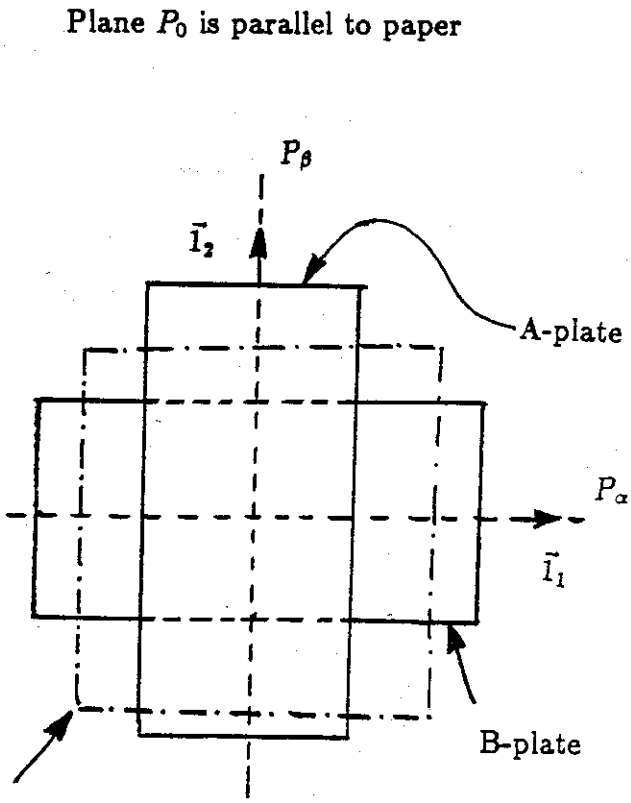

Figure 14. $D_{2,t}$ group
$(N_A = N_B + 1)$
Type A plate on top
Type A plate on bottom

8 Elements of $D_{2,d}Group$

1. identity (1)
2. C_2 rotation about $\vec{1}_0$
3. C_2 rotation about $\vec{1}_1$
4. C_2 rotation about $\vec{1}_2$
5. reflection through plane $P_\alpha(R_\alpha)$
6. reflection through plane $P_\beta(R_\beta)$
7. $\pi/2$ rotation & reflection through plane P_0
8. $3\pi/2$ rotation & reflection through plane P_0

8 Elements of $D_{2,t}Group$

1. identity (1)
2. C_2 rotation about $\vec{1}_0$
3. C_2 rotation about $\vec{1}_1$
4. C_2 rotation about $\vec{1}_2$
5. reflection through P_0 or P_α or P_β
6. $\pi/2$ rotation & reflection through P_0 or P_α or P_β
7. π rotation & reflection through P_0 or P_α or P_β
8. $\pi/2$ rotation & reflection through P_0 or P_α or P_β

The subscript "d" in $D_{2,d}$ refers to the "diagonal" symmetry planes (between $\vec{1}_1$ and $\vec{1}_2$), and "t" in $D_{2,t}$ simply refers to the "transverse" symmetry plane that is orthogonal to the original 2-fold axis $\vec{1}_0$.

One could extend this type of illustration to D_3 and D_4 as sketched in figures 15 and 16. Here, the shapes of plates can be different and as before we could have $D_{3,d}$ and $D_{3,t}$, and, $D_{4,d}$ and $D_{4,t}$ division as well.

In general a D_N capacitor using circular disks as conductors (can be lossy) and tabs is shown in figure 17. The $D_{N,d}$ symmetry group with 4N elements, and diagonal system of axes is illustrated in figure 18. $D_{N,d}$ also has $N_A = N_B = M$ *i.e.*, the numbers of A and B plates are the same. In the $D_{N,d}$ capacitor, we will have an A plate on top and a B plate at the bottom. Of course 'top' and 'bottom' are indistinguishable and they are used for nomenclature only. Such a dihedral capacitor ($D_{N,d}$) will have 4N elements which are, N rotation elements including identity (i.e., 2π rotation), N elements of reflection through each of P_{greek} plane and 2N rotation reflection elements.

As before, one can also consider $D_{N,t}$ symmetry group indicated in figure 19 where $N_A = N_B + 1$, i.e., the number of A plates is one more than number of B plates. This also has 4N elements which are N rotation, N reflection and 2N rotation reflection elements. In both $D_{N,d}$ and $D_{N,t}$ capacitors, the symmetry planes (P_{greek}) are centered on tabs.

In the ultimate limit of $N \to \infty$, the tabs get smaller and smaller and D_∞ capacitor becomes a parallel array of a circular disk capacitors.

We may now proceed to investigate the D_∞ or the disk capacitor as a radial transmission line. This forms the subject of the following section.

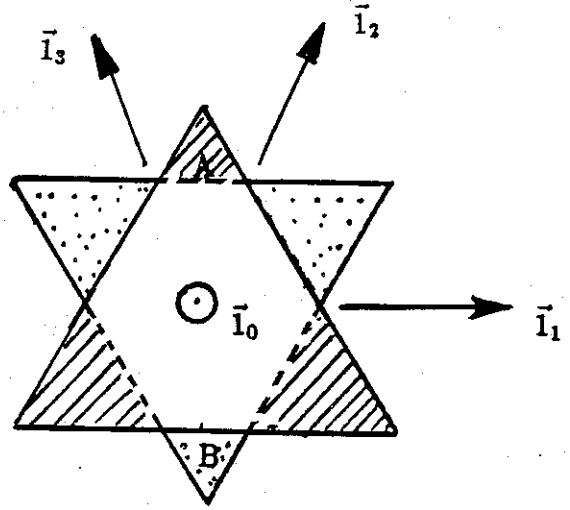

Figure 15. $D_{3,t}$ or $D_{3,d}$, dihedral symmetry group with 12 elements (shapes of plates are not unique)

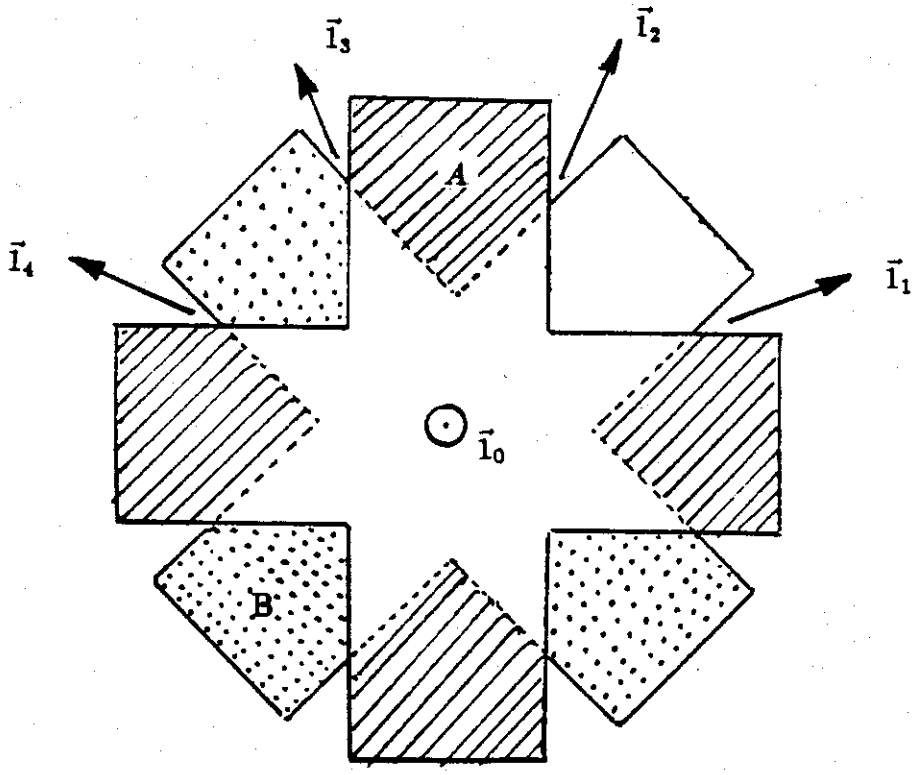

Figure 16. $D_{4,t}$ or $D_{4,d}$, dihedral symmetry group with 16 elements (shapes of plates are not unique)

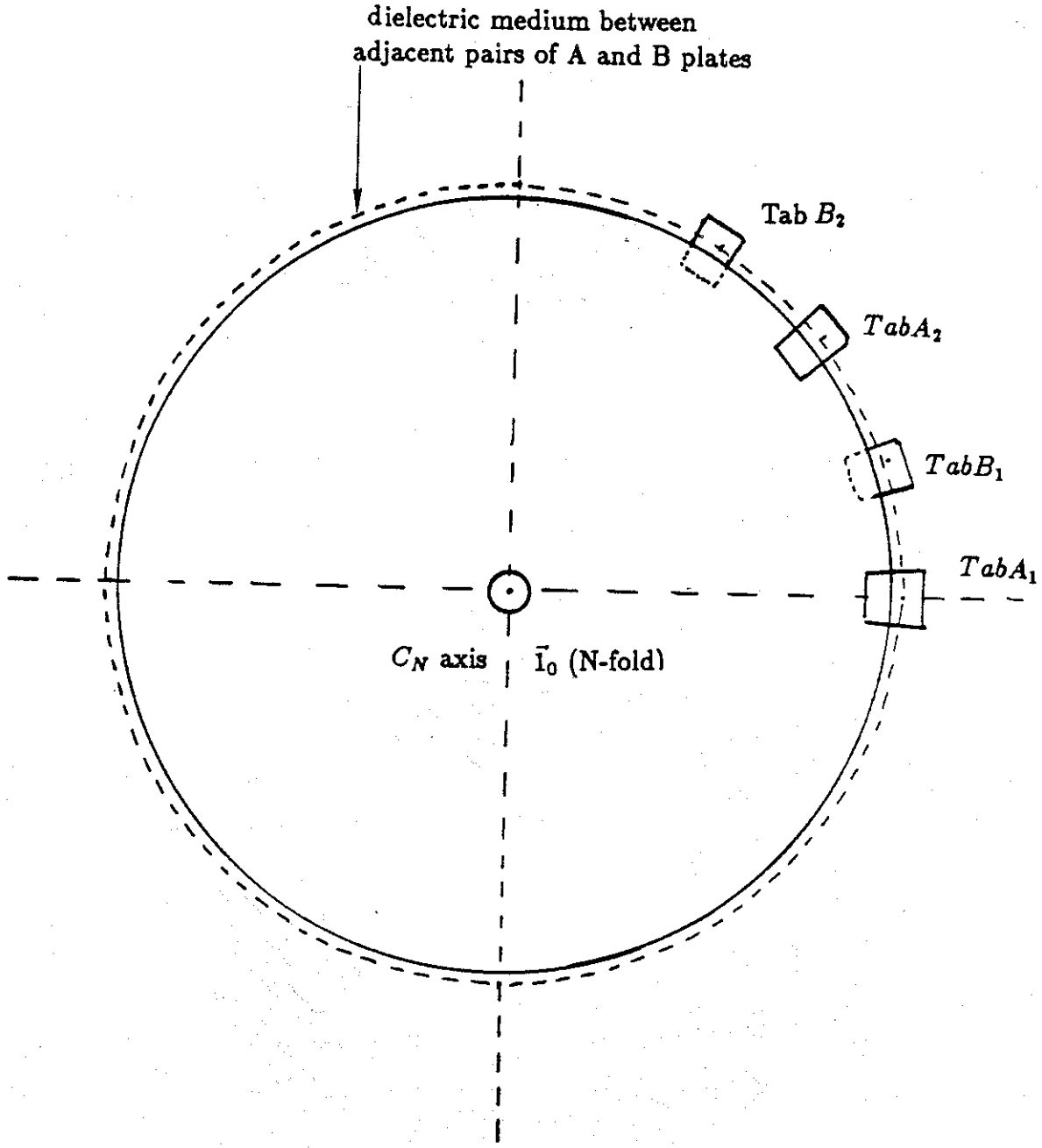

Figure 17. Capacitor belonging to the dihedral D_N symmetry group

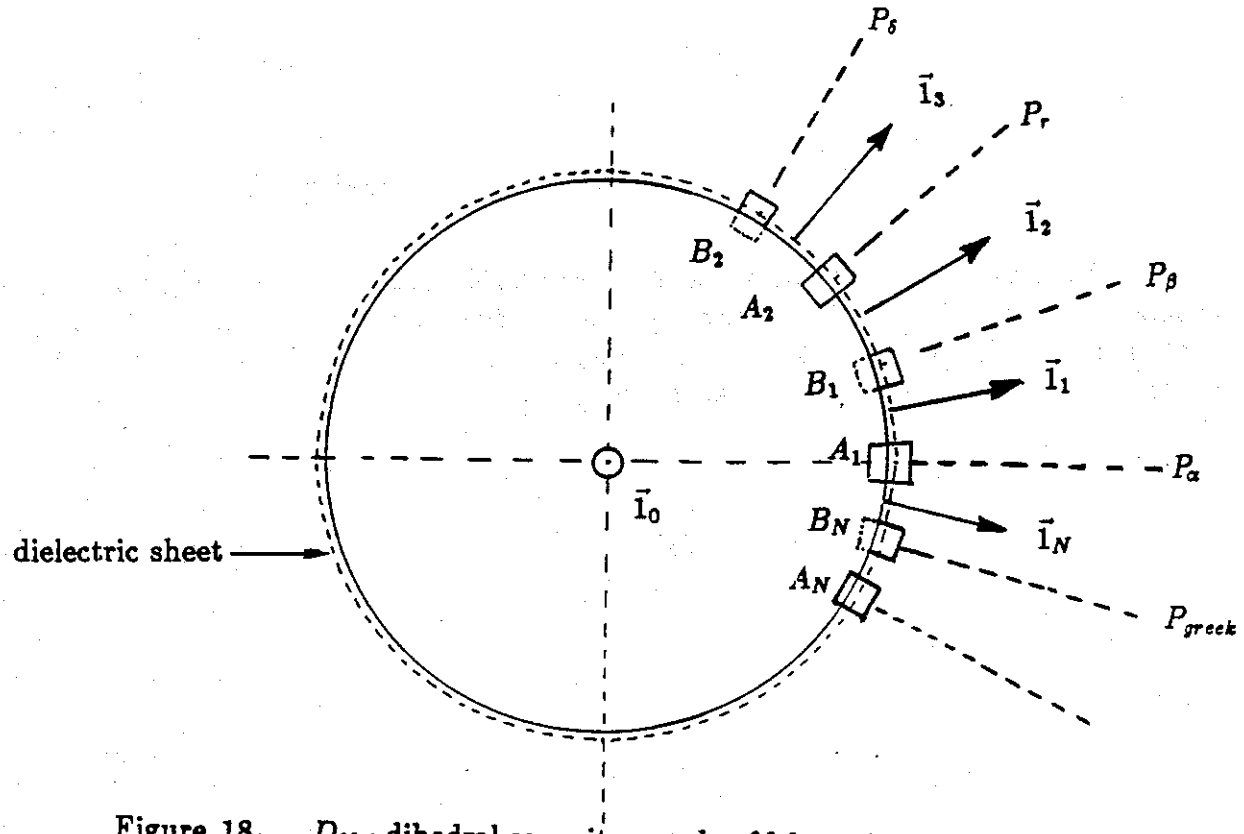

Figure 18. $D_{N,d}$ dihedral capacitor made of M number of circular A and B plates each, with tabs

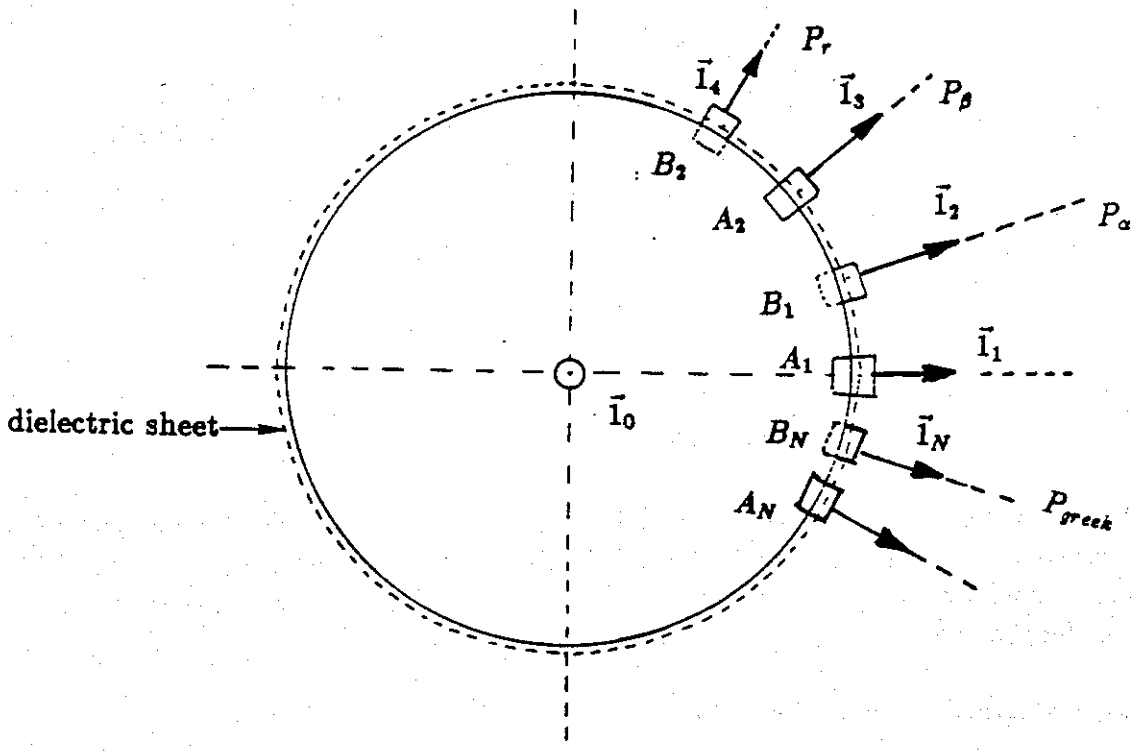

Figure 19. $D_{N,s}$, dihedral capacitor made of N_A number of circular A and $(N_A - 1)$ number of circular B-plates, with tabs

7. Radial-Transmission in a D_∞ Capacitor.

A D_∞ capacitor is basically an array of circular disk capacitors, one element of which is shown in figure 20. It can be analyzed as a radial transmission line where the propagation is radially out from the center along the cylindrical radius coordinate Ψ. The telegrapher's equations for the radial transmission line are given by

$$\frac{d\tilde{V}}{d\Psi} = -Z'\tilde{I} \tag{21}$$

$$\frac{d\tilde{I}}{d\Psi} = -Y'\tilde{V} \tag{22}$$

where

$$Z' \equiv \text{series impedance per unit radial length}$$

$$\equiv sL' + \frac{2Z_s}{2\pi\Psi} \tag{23}$$

$$Y' \equiv \text{shunt admittance per unit radial lengths}$$

$$= sC' \tag{24}$$

and

$$L' = \frac{\mu_0\, d}{2\pi\Psi} \; ; \; C' = \varepsilon\frac{2\pi\Psi}{d} \tag{25}$$

where d is the separation between disks.

In the radial transmission line of figure 20, the direction of wave propagation is the radial coordinate Ψ. A set of cylindrical coordinates (Ψ, ϕ, z) is defined in figure 20. We have considered an incremental length of the transmission line, which is the ring-shaped region of length $\Delta\Psi$.

The telegrapher's equations above apply to this radial transmission line.

In the above equations, we also have

$$\gamma = \sqrt{Z'Y'} = s\sqrt{\mu_0\varepsilon}\left[1 + \frac{2\tilde{Z}_s}{s\mu_0 d}\right]^{\frac{1}{2}} \tag{26}$$

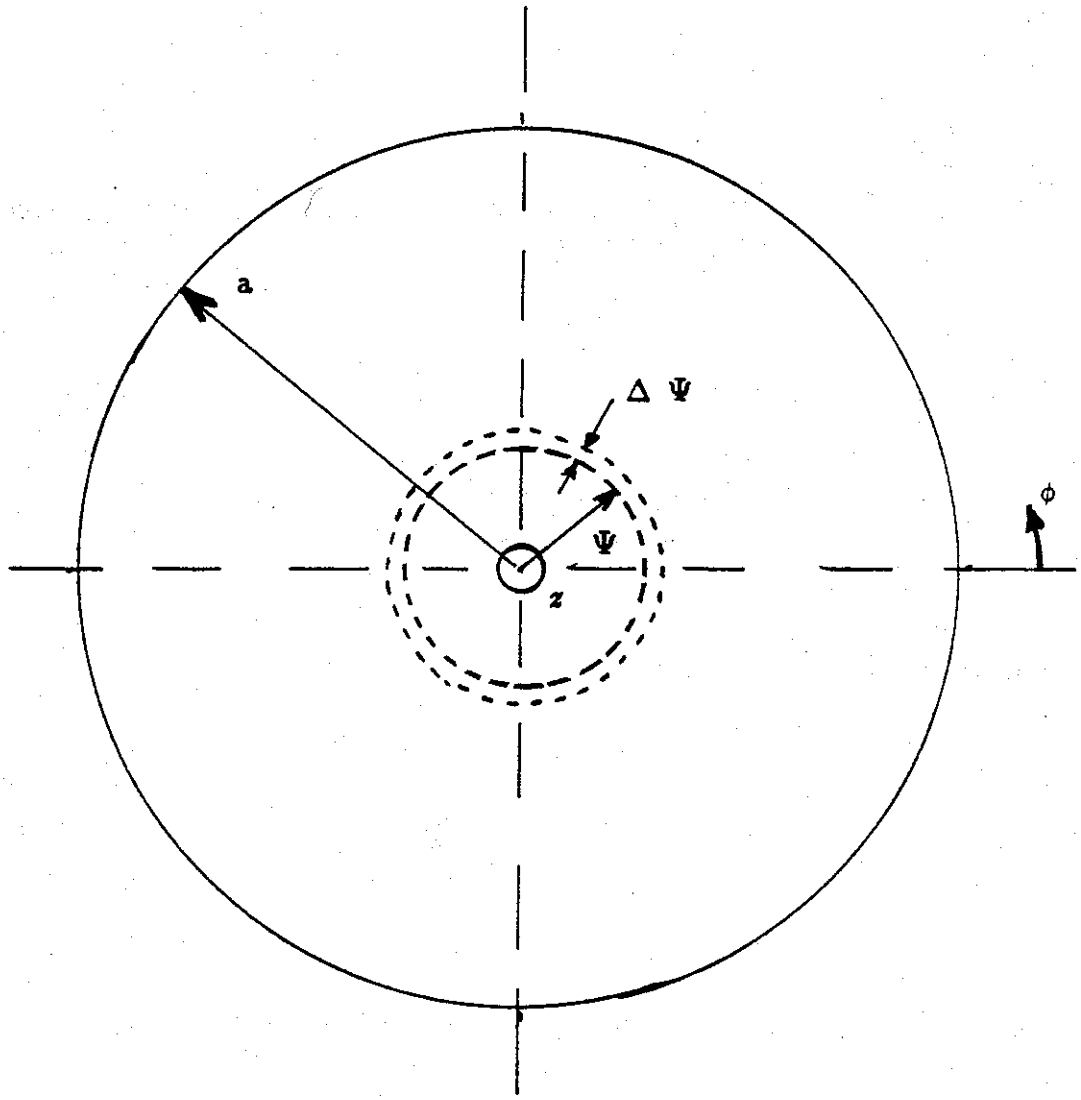

Figure 20. **Disk capacitor and cylindrical coordinates (Ψ, ϕ, z) for analyzing radial transmission**

$$\tilde{Z}_c = \sqrt{\frac{Z'}{Y'}} = \frac{d}{2\pi\Psi}\sqrt{\frac{\mu_0}{\epsilon}}\left[1+\frac{2\tilde{Z}_s}{s\mu_0 d}\right]^{\frac{1}{2}}$$

$$= \frac{\sqrt{Z'Y'}}{Y'} = \frac{\gamma}{Y'} = \frac{\gamma d}{s\epsilon 2\pi\Psi} \tag{27}$$

The telegrapher's equations (20) and (21) may be combined into a single second order differential equation for $\tilde{I}$ or $\tilde{V}$ leading to

$$\frac{1}{\gamma^2}\frac{d^2\tilde{V}}{d\Psi^2} + \frac{1}{\gamma^2}\frac{1}{\Psi}\frac{d\tilde{V}}{d\Psi} - \tilde{V} = 0 \tag{28}$$

$$\frac{1}{\gamma^2}\frac{d^2I}{d\Psi^2} - \frac{1}{\gamma^2}\frac{1}{\Psi}\frac{d\tilde{I}}{d\Psi} - \tilde{I} = 0 \tag{29}$$

The solutions to the above Bessel equations are

$$\tilde{V}(s,\Psi) = V_0\, I_0(\gamma\Phi) \tag{30}$$

$$\tilde{I}(s,\Psi) = -\frac{V_0}{Z_C}\, I_1(\gamma\Phi) \tag{31}$$

where I_0 and I_1, are modified Bessel functions. Note that since the origin ($\Psi = 0$) is in the range of interest K_0 and K_1 are absent from the solution.

Since $\tilde{I}$ is in the direction of increasing Ψ

$$\tilde{Z}_{in} = -\frac{\tilde{V}_{(s,a)}}{\tilde{I}_{(s,a)}} = V_0\tilde{Z}_c\frac{I_0(\gamma a)}{I_1(\gamma a)}$$

$$= \frac{d}{2\pi a\epsilon}\,\frac{\gamma}{s}\,\frac{I_0(\gamma a)}{I_1(\gamma a)} \tag{32}$$

In the special case of $s = j\omega$ and $\gamma = jk$, the above expression reduces to

$$\tilde{Z}_{in} = \frac{d}{2\pi a\varepsilon}\,\frac{k}{\omega}\,\frac{J_0(ka)}{jJ_1(ka)}$$

$$= \frac{d}{j2\pi a}\sqrt{\frac{\mu_0}{\varepsilon}}\,\frac{J_0(ka)}{J_1(ka)} \tag{33}$$

In the above equation, which incidentally can also be derived by a wave analysis, d is the separation between the disks, a is the radius of the disk, μ_0 and ε are the constitutive parameters of the dielectric medium between the disks and the propagation constant k is given by

$$k = \omega\sqrt{\mu_0\varepsilon}\left[1+\frac{2\tilde{Z}_s}{j\omega\mu_0 d}\right]^{\frac{1}{2}} \quad \text{(for lossy case)} \tag{34}$$

$$k = \omega\sqrt{\mu_0\varepsilon} \quad \text{(for lossless case)} \tag{35}$$

Ideally the input impedance is $\tilde{Z}_{ideal} = (j\omega C)^{-1}$ and hence we can define a factor ς as follows

$$\varsigma = \frac{\tilde{Z}_{in}}{\tilde{Z}_{ideal}} = j\omega C\,\tilde{Z}_{in}$$

$$= j\omega C\,\frac{d}{j2\pi a}\sqrt{\frac{\mu_0}{\varepsilon}}\,\frac{J_0(ka)}{J_1(ka)} \tag{36}$$

$$= j\omega\left(\frac{\varepsilon\pi a^2}{d}\right)\,\frac{d}{j2\pi a}\sqrt{\frac{\mu_0}{\varepsilon}}\,\frac{J_0(ka)}{J_1(ka)}$$

$$= \left(\frac{ka}{2}\right)\frac{J_0(ka)}{J_1(ka)} \tag{37}$$

This function ς is shown plotted in figure 21 for the lossless case, meaning that the circular disks are made of perfect conductors. It is obvious that at dc, $\varsigma = 1$ and it goes through a zero at ka = 2.405 and it has an unwanted open-circuit resonance at ka $\simeq$ 3.83 which is the first zero of J_1. The short-circuit resonances, which are zeros of J_0 are acceptable in the sense that the capacitor behaves like an ideal short circuit. The first

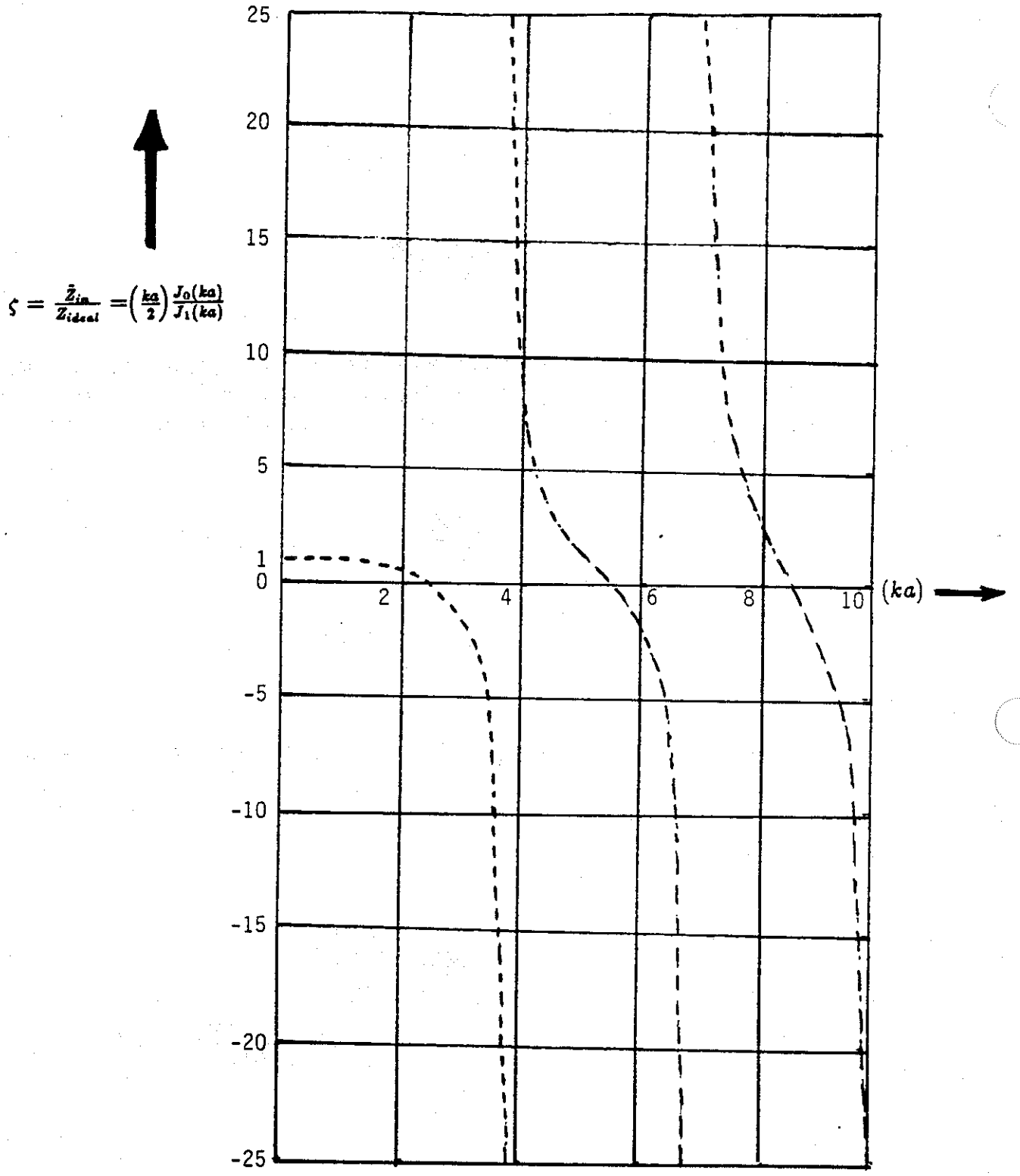

Figure 21. Normalized input impedance of a circular disk (or D_∞ - dihedral) capacitor

open-circuit resonance occurring at ka = 3.83 limits the high-frequency performance of such capacitors. Since there is no propagation at this and higher open-circuit resonance frequencies.

The first open-circuit resonance occurs when

$$ka = \frac{\omega}{c}\sqrt{\epsilon_r}\, a \simeq 3.83 \tag{38}$$

or

$$\begin{aligned} f_r &\equiv 1^{st} \text{ shunt resonant frequency} \\ &\cong \frac{3.83 \times c}{2\pi a\sqrt{\epsilon_r}} \end{aligned} \tag{39}$$

or

$$\begin{aligned} \lambda_r &\equiv \text{first open-circuit resonant wavelength} = \frac{2\pi}{ka} \times a \\ &\simeq \frac{2\pi a}{3.83} \simeq 2.45a \end{aligned} \tag{40}$$

Hence, the first open-circuit resonant wavelength (in the dielectric medium) is larger than the diameter. This indicates to keep λ_r small (or higher frequency performance) one has to make "a" small and ϵ_r large. Note that so far the discussion has been for the lossless situation and if losses are present the propagation constant k becomes

$$k = \omega\sqrt{\mu_0\epsilon}\left[1 + \frac{2Z_s}{j\omega\mu_0 d}\right]^{\frac{1}{2}} \tag{41}$$

with

$$\begin{aligned} Z_s &\equiv \text{surface impedance of the disk} \simeq \sqrt{\frac{j\omega\mu}{\sigma}} \\ &= (1+j)\sqrt{\frac{\omega\mu}{2\sigma}} \end{aligned} \tag{42}$$

For the lossy case, we then have

$$\varsigma = \frac{\tilde{Z}_{in}}{\tilde{Z}_{ideal}} = \left(\frac{ka}{2}\right)\frac{J_0(ka)}{J_1(ka)} \tag{43}$$

where

$$k = \omega\sqrt{\mu_0\varepsilon}\left[1+\frac{1-j}{d}\sqrt{\frac{2\mu_r}{\omega\mu_0\sigma}}\right]^{\frac{1}{2}}$$

$$= \omega\sqrt{\mu_0\varepsilon}\left[1+\mu_r(1-j)\frac{d_s}{d}\right]^{\frac{1}{2}} \tag{44}$$

with d_s being the skin depth in the lossy disk.

As in the case of the transmission line model of the 2-strip capacitor, the losses in the disk capacitor also damp out the unwanted resonance.

Furthermore, we wish to bound $\tilde{Z}_{in}$ near the shunt resonance, so it is small compared with the load impedance that the capacitor is designed to drive. To do this, one can expand (43) around the unwanted resonance

$$k = k_0 + \Delta k \tag{45}$$

This leads to $\tilde{Z}_{in}$ at k_0, given by

$$\tilde{Z}_{in} = \frac{d}{j2\pi a\varepsilon}\,\frac{k}{\omega}\,\frac{1}{\Delta(ka)} \tag{46}$$

From (44), we have

$$ka = \omega\ a\sqrt{\mu_0\varepsilon}\left[1+\mu_r(1-j)\frac{d_s}{d}\right]^{\frac{1}{2}} \tag{47}$$

Now consider $\Delta(ka)$

$$\Delta(ka) = ka - k_0 a \tag{48}$$

For $\mu_r\frac{d_s}{d} \ll 1$, we can write

$$ka \simeq \omega\ a\sqrt{\mu_0\varepsilon}\left[1+\mu_r\frac{(1-j)}{2}\frac{d_s}{d}\right] \tag{49}$$

and

$$\Delta(ka) \simeq \omega\ a\sqrt{\mu_0\epsilon}\ \left[1+\mu_r\frac{(1-j)}{2}\frac{d_s}{d}\right] - k_0 a \tag{50}$$

Now,

$$\begin{aligned}\tilde{Z}_{in} &= \frac{d}{j2\pi a\varepsilon}\ \frac{k}{\omega}\ \frac{J_0(ka)}{J_1(ka)} \\ &\simeq \frac{d}{j2\pi a^2\varepsilon}\ \frac{ka}{\omega}\ \frac{1}{\Delta(ka)}\end{aligned} \tag{51}$$

Substituting (50) into (51),

$$\begin{aligned}\tilde{Z}_{in} &= \frac{d}{j2\pi a^2\varepsilon}\ a\sqrt{\mu_0\epsilon}\ \left[1+\mu_r(1-j)\frac{d_s}{d}\right]^{\frac{1}{2}}\ \frac{1}{\Delta(ka)} \\ &\simeq \frac{d}{j2\pi a}\sqrt{\frac{\mu_0}{\varepsilon}}\ \frac{1}{\Delta(ka)}\end{aligned} \tag{52}$$

So, one can consider $\Delta(ka)$. In magnitude this is minimized at

$$\omega\ a\sqrt{\mu_0\epsilon}\ \left[1+\frac{\mu_r}{2}\ \frac{d_s}{d}\right] \simeq k_0 a \tag{53}$$

showing a slight lowering of the resonant frequency (extra inductance). At this frequency ($\omega \simeq \omega_0$ with slight correction)

$$\Delta(ka) \simeq -j\frac{\mu_r}{2}\ \frac{d_s}{d} \tag{54}$$

and

$$\begin{aligned}\tilde{Z}_{in} &\simeq \frac{d}{2\pi a}\sqrt{\frac{\mu_0}{\varepsilon}}\ \frac{2}{\mu_r}\ \frac{d}{d_s} \\ &= Z_0\frac{1}{\sqrt{\mu_r\varepsilon_r}}\ \frac{d}{a}\sqrt{\frac{f_0\mu_0\sigma d^2}{\pi}}\end{aligned} \tag{55}$$

which is real and positive as required. This expression gives the local maximum of $\tilde{Z}_{in}$ at the first open-circuit resonance f_0.

Let us assume some typical numbers for illustrative purposes.

$$a = 0.075m, \varepsilon_r = 6,\ d = 66\mu m,\ \sigma = 3.57 \times 10^7\ S/m, \mu_r = 1 \text{ (aluminum foils)}$$

$$f_0 \simeq \frac{3.83c}{2\pi a\sqrt{\varepsilon_r}} \simeq 1GHz \tag{56}$$

$$\tilde{Z}_{in}(at f_0) \simeq Z_0 \frac{1}{\sqrt{\mu_r \varepsilon_r}} \frac{d}{a} \sqrt{\frac{f_0 \mu_0 \sigma d^2}{\pi}} \simeq 1.07\Omega \tag{57}$$

which is indeed a considerable improvement. The capacitance C of such a disk capacitor is given by

$$C \simeq \varepsilon_0 \varepsilon_r \frac{\pi a^2}{d} = \frac{1}{36\pi \times 10^9} \times \frac{6 \times \pi \times (0.075 \times 0.075)}{66 \times 10^{-6}} \simeq 14.2nF \tag{58}$$

If one constructs such a capacitor stack say with $N_A = N_B = 50$, then one has $N_0 = N_A + N_B - 1$ to be the total number of capacitors in the stack. Thus the net impedance of the capacitor stack is

$$\tilde{Z}_C = \frac{1}{N_0} \tilde{Z}_{in} \tag{59}$$

and in the above numerical example, the net impedance at the unwanted resonance then becomes,

$$\tilde{Z}_{in} \simeq \frac{1.07\Omega}{100} = 10.7m\Omega \text{ (at resonance)} \tag{60}$$

The total stack capacitance is given by

$$C_{stack} = 100 \times C \simeq 1420nF = 1.42\mu F \tag{61}$$

and the normalized $\tilde{Z}_{in} \equiv \varsigma = j\omega C_{stack} \tilde{Z}_{in}$ at resonance is now given by

$$\varsigma = \tilde{Z}_{in} \left| j\omega c_{st} \right| \simeq \omega\ C_{stack} \tilde{Z}_{in} \text{ (at resonance)} \simeq 95.5 \tag{62}$$

in place of infinity value of ς at resonance.

This is already a vast improvement. Further improvements, i.e., damping of resonance is possible by using even lossier metals.

Since we have just introduced the topic of stacking the elemental capacitors, we may describe this process in greater detail in the following section, and especially look into the symmetry group classification of the stacked capacitors. It would indeed be desirable to preserve the group-symmetric properties even after stacking.

8. Tab Outputs for D_N Capacitor

D_N capacitors have two versions as described earlier. They are $D_{N,d}$ and $D_{N,t}$ of figures 18 and 19 respectively. Recall that there are N_A number of A disks (or plates) and N_B number of B disks (or plates) and that $N_A = N_B$ for $D_{N,d}$ and $N_A = N_B + 1$ for $D_{n,t}$ symmetry groups, which are both dihedral. Each A type disk has N tabs and each B type disk has N tabs, that line up. In other words all of the tabs on A type disks end up on each other and similarly all of the B-disk tabs end up on each other while interleaved between the A-disk tabs. The tabs are then connected together so that there are N sets of A-disk tabs and N sets of B-disk tabs. At this point one has 2 options for bending the tabs. The bending of tabs up or down is essential for stacking and the two options are, (a) A-tabs up and B-tabs down and (b) B-tabs up and A-tabs down.

It is best to illustrate the above process of tab bending with an example of $D_{2,d}$ and $D_{2,t}$ dihedral capacitors.

$D_{2,d}$ and $D_{2,t}$ capacitors are shown in figures 22 and 23, along with their principal 2-fold axis $\vec{1}_0$, a set of orthogonal axes $\vec{1}_1$ to $\vec{1}_4$ and the symmetry planes $P_\alpha, P_\beta, P_\gamma, P_\delta$.

Each of the A and B disks (shape itself is not relevant for this discussion) has 2 tabs denoted by A_1, A_2 for the A type disks and B_1, B_2 for the B- type disks. When N_A and N_B number of such disks are stacked with appropriate dielectric medium between every A and B disk, we have a stacked capacitor where all corresponding tabs A_1, A_2, B_1, and B_2 line up and get interconnected. The two options of tab bending are illustrated in figure 24. These two options can be applied to both $D_{2,d}$ and $D_{2,t}$. In the case of $D_{2,d}$ A and B plates are indistinguishable, i.e., A and B plates are interchangeable because rotation is still possible about $\vec{1}_1$ and $\vec{1}_2$ to make the interchange, and the interconnection of stacked capacitors also lead to $D_{2,d}$ point-symmetry group. The term "point-symmetry group" simply means, that all transformations of this symmetry group leave one point fixed in the body.

However, in the case of $D_{2,t}$ the bending of tabs leads to two distinguishable stacks since there are no rotation symmetries about $\vec{1}_1$ and $\vec{1}_2$. When such stacks are interconnected, the resulting capacitor is found not to be a $D_{2,t}$ capacitor. This is the direct consequence of the fact that in a $D_{2,t}$ capacitor, we have one more A plates than B plates.

The above illustration leads us to conclude that $D_{2,d}$, or in general $D_{N,d}$ is the preferred capacitor since it preserves the group-symmetric property when stacked units are themselves "stacked" or interconnected. In contrast, a stack of stacked $D_{2,t}$ or in general $D_{N,t}$ is not a $D_{N,t}$. For clarity of nomenclature, we heretofore call a single capacitor as an elemental capacitor. When N_C number of them are stacked to form a unit it is called a capacitor stack or a unit capacitor. Unit capacitors are then series connected to form a column capacitor. So an elemental capacitor is the basic building block, unit capacitor are

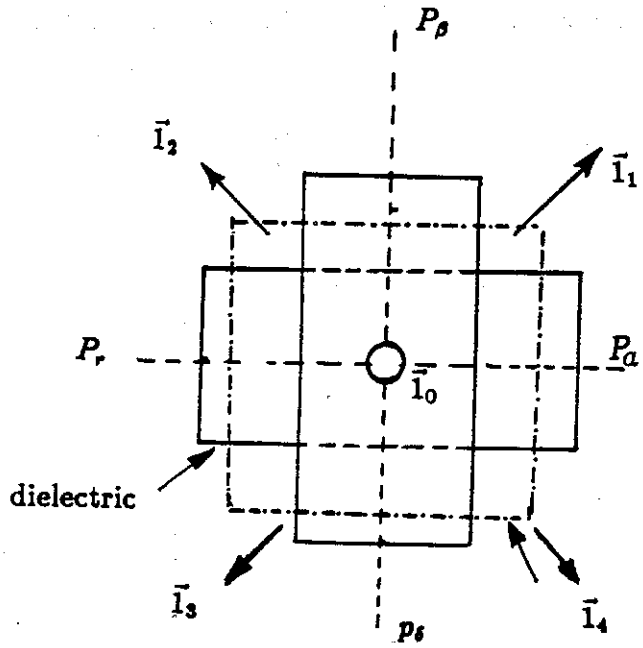

Figure 22. $D_{2,d}$ capacitor ($N_A = N_B$)

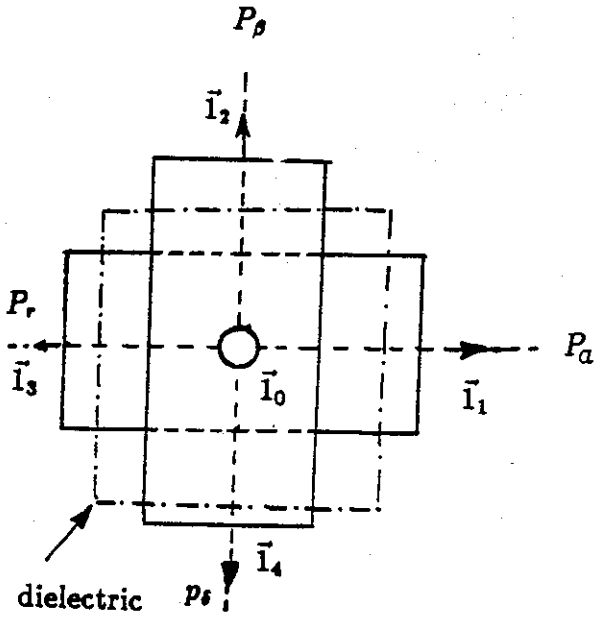

Figure 23. $D_{2,t}$ capacitor ($N_A = N_B + 1$)

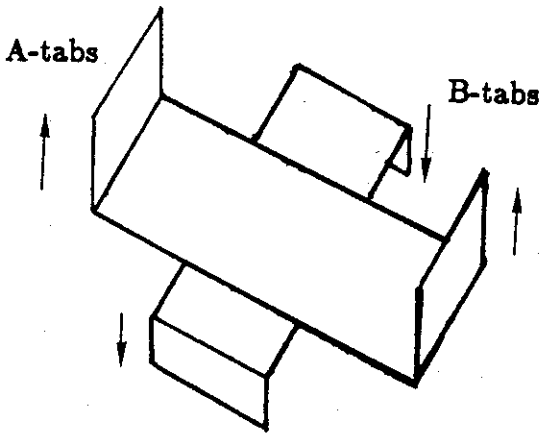

a) A-tabs

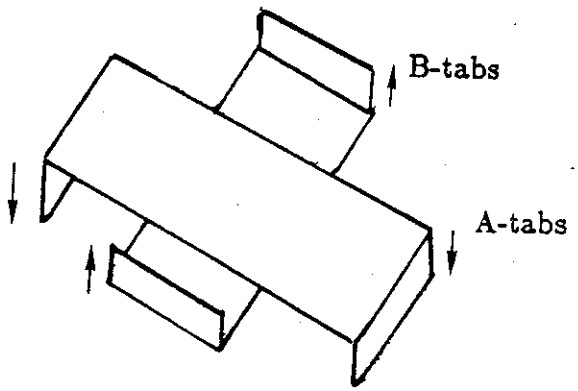

b) B-tabs

Figure 24. Two ways of bending the tabs, both of which can be applied to $D_{2,d}$ and $D_{2,t}$ above

the next level building blocks and the column capacitor is the end product (like a peaking capacitor arm).

We have referred to making a column capacitor by interconnecting unit capacitors above and this subject is pursued in greater detail in the following section.

9. Combining $D_{N,d}$ Unit Capacitors.

Let us say that each elemental capacitor, i.e., capacitance of one each of A and B plates separated by a dielectric medium is C_0. C_0 is roughly (truly at low frequencies) given by the product of the permittivity of the medium and plate area divided by the plate spacing. When N_A number of A plates and N_B number of B plates are stacked to form a unit capacitor, the capacitance value C of the stack or unit capacitor is given by

$$C = [\#\text{of foils} - 1]\, C_0 = N_0 C_0 \tag{63}$$

where N_0 represents the number of dielectric "sheets". There is one dielectric sheet, which itself may be a composite of layered dielectric sheets, between all pairs of adjacent A and B plates. Consequently, one has N_0 number of elemental capacitors in parallel in a unit capacitor. When N_C number of unit capacitors are series connected to form a column capacitor, the resultant column capacitance is

$$\begin{aligned} C_c &\equiv \text{net column capacitance} \\ &= \frac{C}{N_c} = \frac{N_0 C_0}{N_c} \end{aligned} \tag{64}$$

In other words, in a column capacitor, there are N_0 number of elemental capacitors in parallel and N_c number of elemental capacitors in series. N_c can be greater than, equal to or less than N_0 so the column capacitance may be greater than, equal to or less than elemental capacitance. This is purely a function of intended application. The voltage across a unit capacitor is N_c^{-1} times the total voltage across the column, all things being equal.

Furthermore N_c can be odd or even and a column of $D_{N,d}$ capacitors is a $D_{N,d}$ if N_c is odd. One could also show that a column of $D_{N,d}$ capacitors is a $D_{N,t}$ if N_c is even. The "columning" or stringing of $D_{N,d}$ capacitors is schematically shown in figure 25 for the special case of $D_{2,d}$. As we have noted earlier $D_{N,d}$ preserves the symmetry group upon bending of the tabs, which are essential. Therefore, $D_{N,d}$ is the preferred dihedral capacitor. Depending upon N_c (number of $D_{N,d}$s in a string) being odd or even, the column itself is respectively $D_{N,d}$ or becomes $D_{N,t}$. Figure 25 can also be redrawn to show the principal axes and this has been sketched in figure 26. In figure 26, we have strung together $D_{2,d}$ capacitors showing the N-fold (N=2) C_2 axis labelled $\vec{1}_0$. This is also the axis of column capacitor. The secondary set of orthogonal axes in each $D_{2,d}$ are indicated. They are parallel to each other and uniformly spaced from one $D_{2,d}$ to the next. In figure 27a, we consider a special case of $N_c \equiv$ even number $= 8$. The principal 2-fold axis $\vec{1}_{0_A} = \vec{1}_0$ and the secondary C_2 rotation axes $\vec{1}_{1_A}$ and $\vec{1}_{2_A}$ which are orthogonal to $\vec{1}_{0_A}$

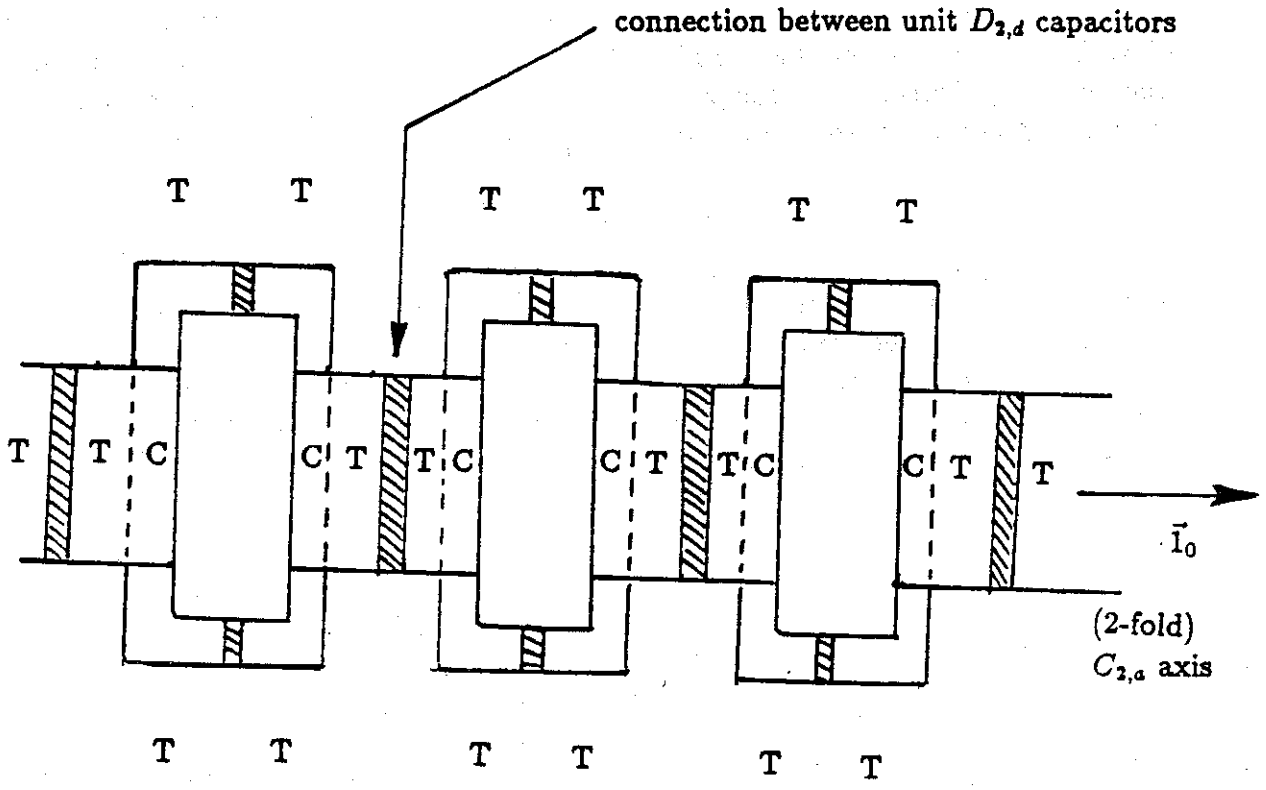

Figure 25. Stringing of $D_{2,d}$ capacitors to form a column capacitor

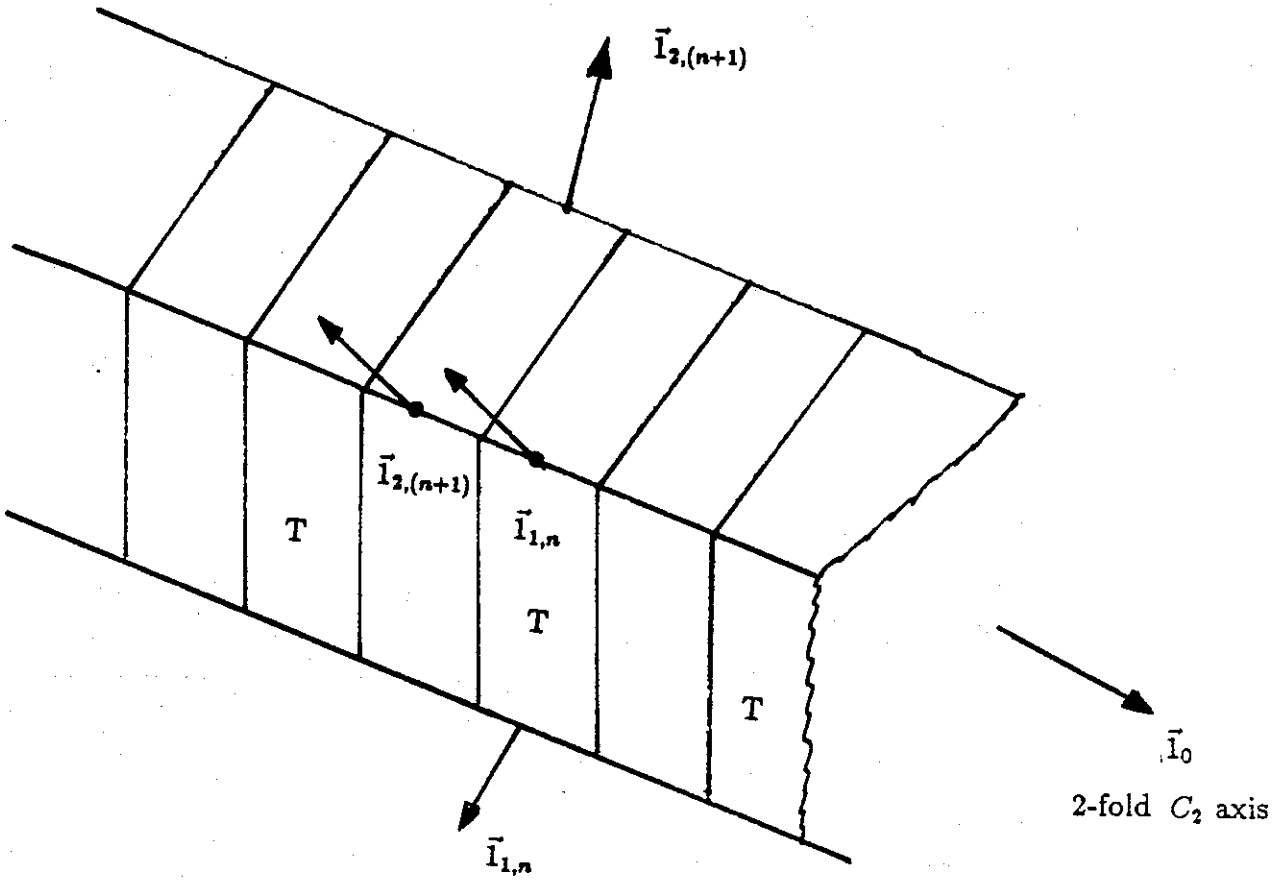

Figure 26. Column of $D_{2,d}$ capacitors

Note: Each $D_{2,d}$ unit capacitor is represented by a square box with tab connections on mating square faces between adjacent units.

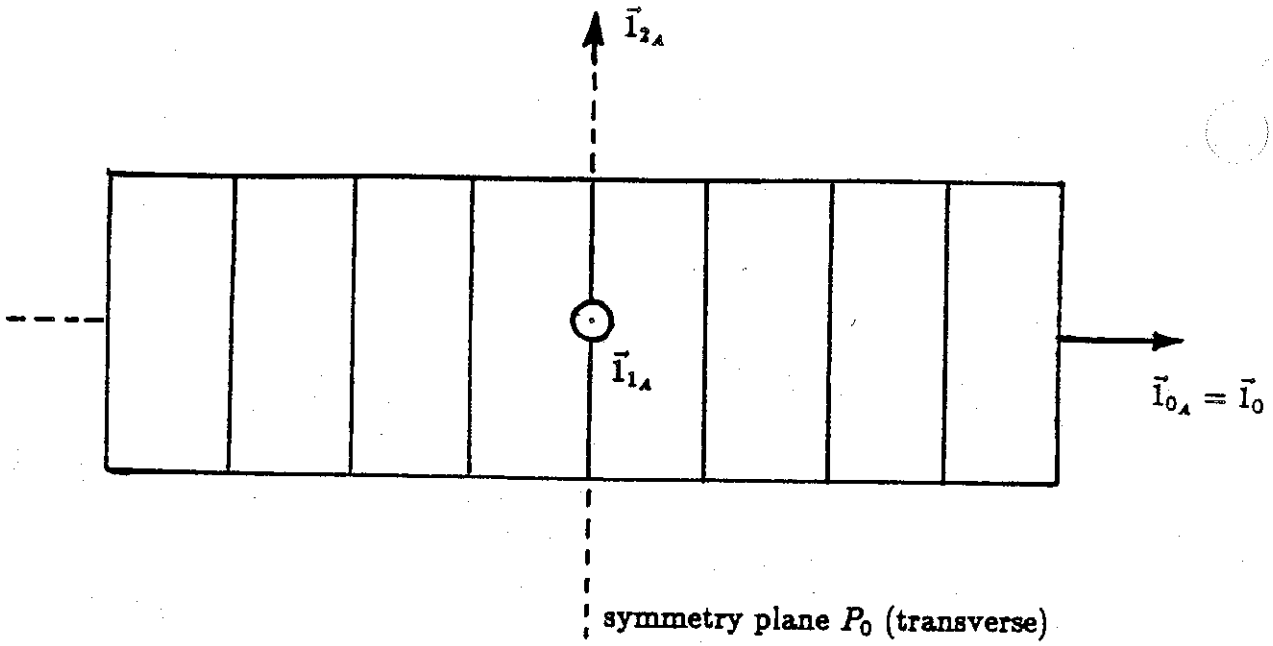

a) Case of N_c even (= 8 say) $D_{2,d}$'s resulting in $D_{2,t}$

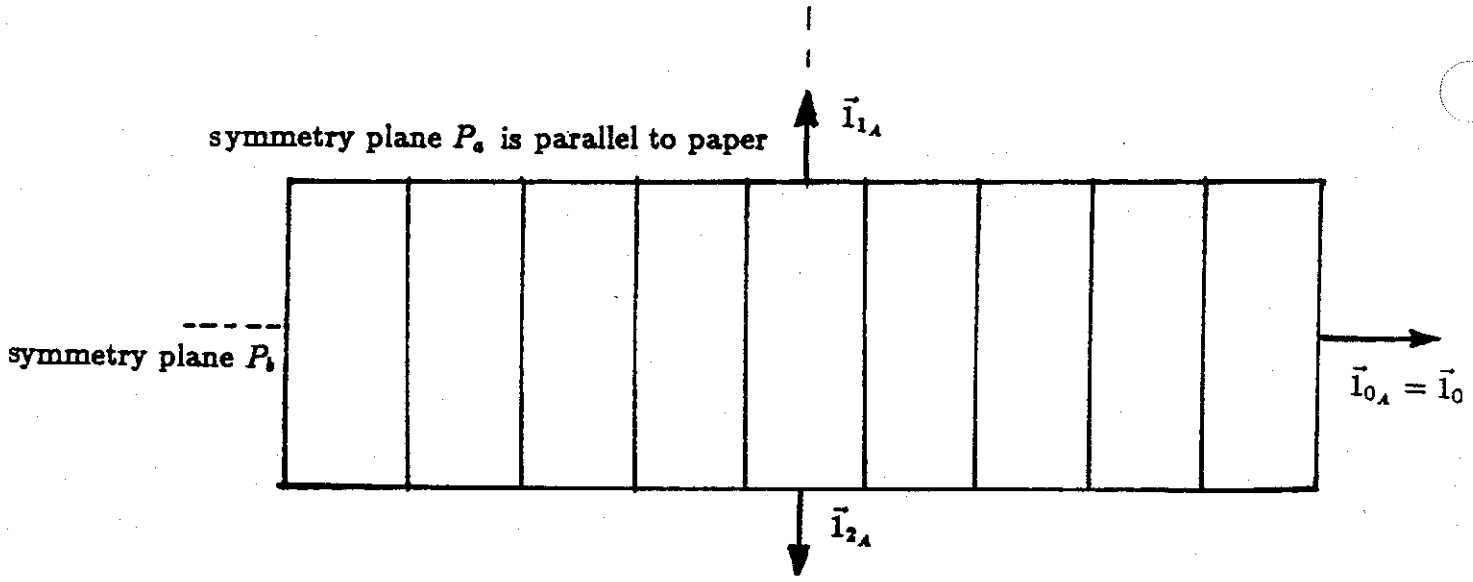

Note that the secondary axes $\vec{I}_{1_A}$ and $\vec{I}_{2_A}$ are 45^0 and 225^0 w.r.t. paper

b) Case of N_c odd (= 9 say) $D_{2,d}$'s resulting in $D_{s,d}$

Figure 27. A column of $D_{2,d}$ capacitors for the two cases of N_c even and odd

are also indicated. For this special case of $N_c = 8$, the resulting column is a $D_{2,t}$ and has 8 elements. In figure 27b, we consider the case of N_c odd (= 9 say). The rotation axes $\vec{1}_{1_A}$ and $\vec{1}_{2_A}$ are along the "diagonals", i.e., at 45° and 225° with respect to the plane of the paper. The symmetry planes P_a and P_b are indicated and the axis of the column is still $\vec{1}_0$. The resulting symmetry group in this case of N_c odd is still $D_{2,d}$.

In conclusion, we remark that the preferred dihedral capacitor is a $D_{N,d}$ which can be strung together to form a column that is either a $D_{N,d}$ or a $D_{N,t}$ depending on whether an odd or even number of unit capacitors are present in a column.

The unit capacitor or a column of unit capacitors (to increase the voltage standoff) can be fabricated in a box-like structure to make a $D_{2,d}$ unit or column capacitors. The unit capacitors themselves can be modular and the interconnection of unit capacitors is uniquely achieved by suitable mechanical design of the box.

10. Concluding Remarks

In designing high frequency capacitors, we have found several useful techniques and the various underlying considerations are listed below:

1. electrical lengths of foils (between tabs) should be kept small
2. the dielectric constant of the medium between the foils should be high
3. multitabs on foils help in increasing the high-frequency performance
4. physical dimensions of an elemental capacitor should be kept small e.g., order of 0.1 m for a useful bandwidth of several hundred MHz, consistent with flat foils as opposed to windings
5. elemental capacitors can be arranged in parallel to form a unit capacitor
6. ways of multiple tabbing of the disk capacitors are illustrated, along with how they are bent to facilitate interconnections
7. higher frequency performance is obtainable by maximizing the symmetry properties of the capacitors (dihedral point - symmetry groups are considered and found suitable for these capacitors)
8. same number of A and B (or + and -) plates are preferred in a stack over the option of having one more A (or +) plate than B plates, i.e., a $D_{2,d}$ unit capacitor is the preferred choice
9. losses in the foils (e.g., lead, iron or carbon coating) help in damping the unwanted resonances
10. unit capacitors are series connected to form a column capacitor

The preferred $D_{2,d}$ unit is quite simple in construction. It comprises of rectangular foils/tabs. The foils and tabs are formed of one piece of metal (or lossy metal). Square shaped dielectric sheets are introduced between adjacent pairs of foils. The $D_{2,d}$ can be fabricated into a square box (and not necessarily cubical) if desired. $D_{2,d}$ unit capacitors may easily be fabricated in future prototype models for experimental investigations.

In concluding this paper, it is emphasized that the design concepts presented here should in future be experimentally optimized. A carefully designed set of experiments of dihedral capacitors at the elemental, unit and column level are recommended for future studies. The resonances of the column capacitor is closely linked to the resonance of the elemental capacitor and hence, we have focussed our attention on designing a better elemental capacitor. Some refinement of these concepts may be in order as experimental results become available. It is evident that a judicious combination of concepts and experimental results will in future lead to optimized high-frequency capacitors.

References

1. C. E. Baum, *"EMP Simulators for Various Types of Nuclear EMP Environments: An interim Categorization"*, Sensor and Simulation Note 240, January 1978 and Joint Special Issue on the Nuclear Electromagnetic Pulse, IEEE Transactions on Antennas and Propagation, Vol. AP-26, No. 1, January 1978, pp. 35–53, and IEEE Transactions on Electromagnetic Compatibility, Vol. EMC-20, No. 1, February 1978, pp. 35–53.

2. I. D. Smith and H. Aslin, *"Pulsed Power for EMP Simulators"*, IEEE Trans., on Antennas and Propagation, Joint Special Issue on the Nuclear Electromagnetic Pulse, Vol., AP-26, Nol. 1, January 1978, pp. 53–59, also in IEEE Trans., on Electromagnetic Compatibility, Vol. EMC-20, No. 1, February 1978, pp. 53–59.

3. R. W. Latham, *"Corrections to the Transmission-Line Parameters of a Coaxial Line when the Center Conductor has Impedance"*, Sensor and Simulation Note 168, March 1973.

4. D. V. Giri and C. E. Baum, *"Theoretical Considerations for Optimal Positioning of Peaking Capacitor Arms about a Marx Generator Parallel to a Ground Plane"*, Circuit and Electromagnetic System Design Notes, Note 33, 26 June 1985.

5. M. Hammermesh, Group Theory and its Application to Physical Problems, Chapters 1 and 2, Addison-Wesley, Reading, MA., 1962.

6. C. E. Baum, *"Interaction of Electromagnetic Fields with an Object which has an Electromagnetic Symmetry Plane"*, Interaction Note 63, 3 March 1971.

7. C. E. Baum, *"A Priori Application of Results of Electromagnetic Theory to the Analysis of Electromagnetic Interaction Data"*, Interaction Note 444, 3 February 1985 and Radio Science, 1987, pp. 1127–1136.

8. D. V. Giri and C. E. Baum, *"Airborne Platform for Measurement of Transient or Broadband CW Electromagnetic Fields"*, Sensor and Simulation Note 284, 22 May 1984, also see the paper with the same title in Electromagnetics, Vol. 8, No. 4, October–December 1988.

9. C. E. Baum, *"Combining RF Sources Using C_N Symmetry"*, Circuit and Electromagnetic System Design Notes, Note 37, 6 June 1989.

10. C. E. Baum, *"SEM Backscattering"*, Interaction Note 476, 19 July 1989.